Spring 5-1-2020

Raman Spectroscopic and Quantum Chemical Investigation of the Effects of Tri-Methylamine N-Oxide (TMAO) On Hydrated Urea, Hydrated Guanidinium, and Hydrogen Bonded Networks

Genevieve Verville

Raman Spectroscopic and Quantum Chemical Investigation of the Effects of Tri-Methylamine N-Oxide (TMAO) On Hydrated Urea, Hydrated Guanidinium, and Hydrogen Bonded Networks

By
Genevieve A. Verville

A thesis submitted to the faculty of the University of Mississippi in partial fulfillment of the requirements of the Sally McDonnell Barksdale Honors College.

Oxford
May 2020

Approved by:

Dr. Nathan I. Hammer (Advisor)

Dr. Ryan C. Fortenberry (Reader)

Dr. Gregory S. Tschumper (Reader)

ACKNOWLEDGEMENTS

Many people at the University of Mississippi have played an important role both in the work presented in the thesis and in my life during my undergraduate career. First, I would like to thank Dr. Nathan Hammer for taking a chance on me three and a half years ago by allowing me to join your research group. I do not believe that I would be where I am today if it was not for your unwavering encouragement, support, and opportunities that you have provided me. To the entire Hammer Research Group, especially April Hardin, Austin Dorris, and Ashley Williams, thank you for supporting me and always pushing me to reach my full potential. I would like to thank the Sally McDonnell Barksdale Honors College for providing me with transformative out-of-classroom experiences that have greatly contributed to my personal growth. To Dr. Gerald Rowland, thank you for always having an open door and caring about me. Words cannot describe how grateful I am to have had you as a professor and a mentor. To Dr. Ryan Fortenberry, thank you for your amazing advice, entertaining stories, and letting me be a part of your class. To my professors and TAs, thank you for your passion and dedication to teaching. Thank you for believing in me, even when I had little faith in myself. To my friends and family, thank you for your endless support, encouragement, and love. Lastly, to the entire Department of Chemistry and Biochemistry, thank you for giving me a place to call home.

ABSTRACT

Trimethylamine N-Oxide (TMAO), guanidinium, and urea are three important osmolytes with their main significance to the biophysical field being in how they uniquely interact with proteins. TMAO is known to stabilize and counteract the destabilizing effects of both urea and guanidinium. The exact mechanisms by which TMAO stabilizes and both guanidinium and urea destabilize folded proteins continue to be debated in the literature. Some studies suggest that solvent interactions do not play a large role in TMAO's stabilizing effects and therefore advocate direct stabilization, whereas others suggest that TMAO counteracts denaturation primarily through an indirect effect of strong solvent interactions. Herein, we use Raman spectroscopy to elucidate the physical interactions between the osmolytes of interest in aqueous solutions to better understand how they interact with each other and affect adjacent hydrogen-bonding networks of water. Comparing experiment to theory yields good agreement, and it was determined that adding TMAO into both an aqueous solution of guanidinium and an aqueous solution of urea induces a blue shift (shift to higher energy) in both urea and guanidinium's H-N-H bending modes, which is indicative of direct interactions between the osmolytes.

TABLE OF CONTENTS

LIST OF TABLES

LIST OF FIGURES

CHAPTER 1

INTRODUCTION TO NONCOVALENT INTERACTIONS

1.1 Types of Bonds

When atoms come close together, electrons in their valence shells can interact with each other, and consequently form a bond.[1] Ionic bonding refers to a bond formed between a non-metal and a metal, where the non-metal is an anion and the metal is a cation.[2] This involves a complete transfer of valence electrons from atom to another.[2] One of the strongest types of bonds present in nature is a covalent bond. A covalent bond forms between two nonmetals.[1-4] Two different types of covalent bonds are nonpolar covalent and polar covalent. Nonpolar covalent bonds are formed between two of the same atoms, or between two atoms with similar electronegativities. Consequently, the number of electrons shared between both atoms are the same.[3] Diatomic molecules, such as H_2, I_2, and Br_2, are common examples of molecules containing nonpolar covalent bonds. On the other hand, polar covalent bonds form between two different atoms with different electronegativities, resulting in an unequal sharing of electrons.[2-4] This unequal sharing of electrons can be characterized by the difference in charges of the two atoms.[2-4] One of the atoms usually possesses a partial negative charge, whereas the

other has a partial positive charge.[2-4] Common examples of molecules with polar covalent bonds are water and hydrochloric acid.

Covalent bonds form largely as a result of electrostatic interactions between the nuclei and the bonding electrons located in the space between the nuclei, resulting in a filled bonding molecular orbital.[5] Additionally, the distance between the two nuclei impacts the stability of the bond formed.[2-4] Valence Bond Theory can be used to further describe the stability of the interaction formed by a covalent bond. Figure 1.1 illustrates the energy of a system for a diatomic molecule as a function of internuclear distance.

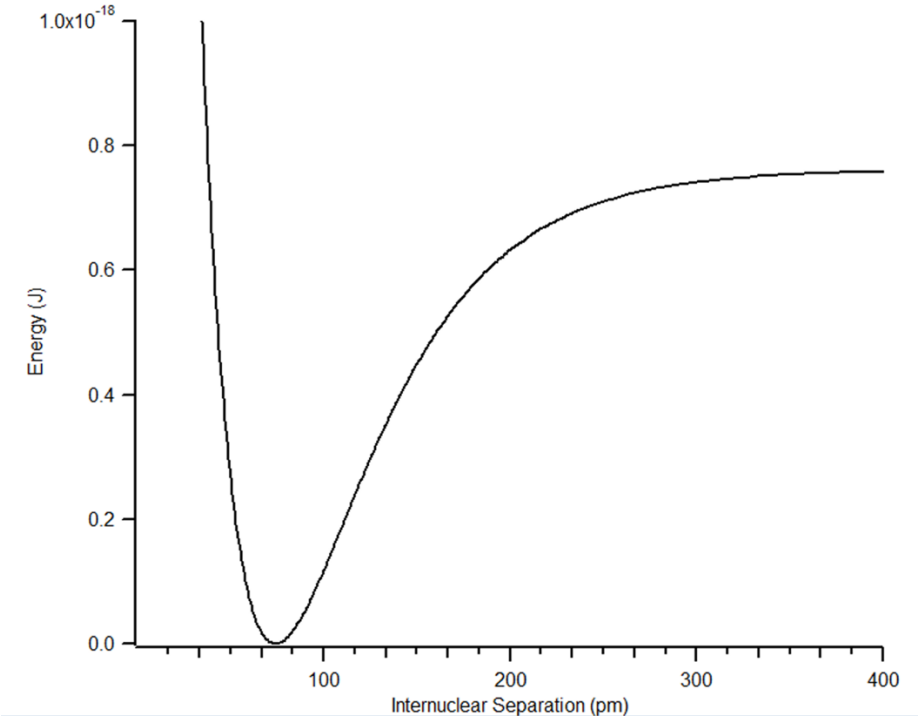

Figure 1.1 Morse Potential of H_2.

When the two atoms are far apart from each other, they do not interact; however, as the atoms move closer together, attractive forces increase as the orbitals overlap with each other, resulting in a decrease in energy.[2-4] As the orbitals become closer together, repulsion between the electrons also increases.[4] At a certain bond distance, the molecule achieves its lower energy conformation, illustrated by the minima shown in Figure 1.1. [2-4] If the distance between the atoms continues to decrease, repulsive forces between the electrons dominate, decreasing its overall stability and increasing the energy.[4]

On the other hand, when molecules interact with each other and no covalent bonds are formed or broken, a molecular cluster is formed.[6] This phenomenon is commonly categorized as noncovalent interactions, and these interactions are significantly weaker than covalent bonds.[6] Nevertheless, these interactions play an important role in stabilizing several important biological macromolecules, namely: DNA and proteins.

1.2 Noncovalent Interactions

Noncovalent interactions can significantly impact a molecular system, and are responsible for biologically relevant phenomena such as pi-stacking, hydrophobic interactions, hydrogen bonding, and metal coordination.[6] Metal coordination plays

an important role in the human body, as heme groups containing iron centers are responsible for delivering oxygen to tissues.[6, 7] Additionally stacking interactions, hydrophobic interactions, and hydrogen bonding all play an important role in maintaining the integrity of DNA's double helix.[6-8] Consequently, elucidating the impact of noncovalent interactions on a system in order to gain insight into its biological function is of utmost importance; however, this can prove to be particularly challenging when using computational methods, such as the methods employed in this work.[6,9,10]

There are several types of noncovalent interactions that are of importance in biological macromolecules, namely, dispersion forces, dipole-dipole, ion-dipole, and hydrogen bonding.[2] Dispersion forces exist within all molecules and atoms, and are caused by the instantaneous dipole that results from the constant movement of electrons.[11] This instantaneous dipole occurs when the electrons are unevenly distributed around the nucleus.[11] These molecules impact neighboring molecules, as the positive end instantaneous dipole attracts the end of the negative end of another molecule's dipole.[2] Moreover, dispersion forces increase with a molecule's size: larger molecules have more dispersion forces, and consequently, have a larger electron cloud.[11] Ion-dipole forces result from the mixture of an ionic molecule (such as NaCl) with a polar compound.[2] Both the positively and negatively charged ions

interact with water, where the positively charged ions interact with the polar compound's negative pole, and the negatively charged ions interact with the positive pole.[2] Dipole-dipole interactions occur between polar molecules, or molecules with a permanently induced dipole.[2] These molecules have an uneven distribution of charge density within the molecule, resulting in each molecule possessing an electron-rich region, and an electron-deficient region.[2,4] This facilitates their interaction with other polar molecules.[2] Hydrogen bonding is a special type of dipole-dipole interaction that occurs when hydrogen atoms are bonded to electronegative atoms such as fluorine, oxygen, or nitrogen.[2]

1.2 Hydrogen Bonding

The concept of hydrogen bonding first emerged in the twentieth century, when Latimer, Rodenbush, and G.N. Lewis sought to describe the properties of water.[12] They first described a hydrogen bond by suggesting that the free pair of electrons on oxygen might have the capability to exert a force on a neighboring hydrogen atom that would bind the molecules together.[12,13] Linus Pauling first coined the term hydrogen bond in 1939, describing it as a hydrogen atom attracted by force to two atoms.[13] However, Pauling described the bond as a result of ionic forces.[13] In 1960, George Pimentel and Aubrey McClellan defined the hydrogen bond as a

bond that exists between a functional group and an atom when there is both evidence of bond formation and that this new bond specifically involves a hydrogen atom.[12,13] Their definition is consistent with the definition for a hydrogen bond commonly used today. In 2011, IUPAC formally defined a hydrogen bond as such: "The hydrogen bond is an attractive interaction between a hydrogen atom from a molecule or a molecular fragment X–H in which X is more electronegative than H, and an atom or a group of atoms in the same or a different molecule, in which there is evidence of bond formation."[14]

Hydrogen bonding plays an important role in the stability of biological macromolecules and processes, such as protein folding and holding DNA together, and in understanding the properties of water as the universal solvent.[15-17] Hydrogen carries a positive charge, while the other more electronegative atom carries a negative charge and possesses a lone pair of electrons.[2,18] The large differences in electron density contributes to the differences in these charges.[2] Although covalent bonds are considered to be one of the strongest types of bond, hydrogen bonding is the strongest intermolecular force.[2]

Hydrogen bonding plays an important role in water's ability to act as a solvent. Water molecules can form a maximum of four hydrogen bonds, with the oxygen atom forming a maximum of two hydrogen bonds, and each hydrogen atom

forming one bond.[19] The arrangement of water molecules and their respective hydrogen bonds is impacted by both temperature and pressure.[19] Water molecules tend to be less ordered at higher temperatures and more ordered at lower temperature.[19]

CHAPTER 2

SPECTROSCOPY

2.1 Principles of Light-Matter Interactions

Spectroscopy is the study of matter through its interactions with light, which can be used to determine molecular properties.[20,21] Light, also known as electromagnetic radiation, acts as both a wave and a particle.[22] This phenomenon is known as wave-particle duality, and thus, it exhibits properties of both waves and particles.[22] Moreover, light is composed of quantized units called photons, meaning that if a molecule absorbs a photon, the electrons in the molecule will be promoted to an excited state.[21] This phenomenon can only occur when the energy of the photon (E) matches the energy between the quantum states.[23] Einstein proposed the theory that light is quantized, and postulated that energy depends on frequency.[23] Since frequency can also be related to wavelength, Equation 2.1 can be used to express the energy of a photon.

$$E = h\nu = \frac{hc}{\lambda} \tag{2.1}$$

In this equation, both h and c are constants, where h is Planck's constant (6.626×10^{-34} Js), and c is the speed of light (3.0×10^{8} m/s). Notably, this equation shows the inverse relationship between frequency and wavelength, and their relationship with energy. The electromagnetic spectrum illustrates the different types of light waves in relation to each other (Fig 2.1).[24]

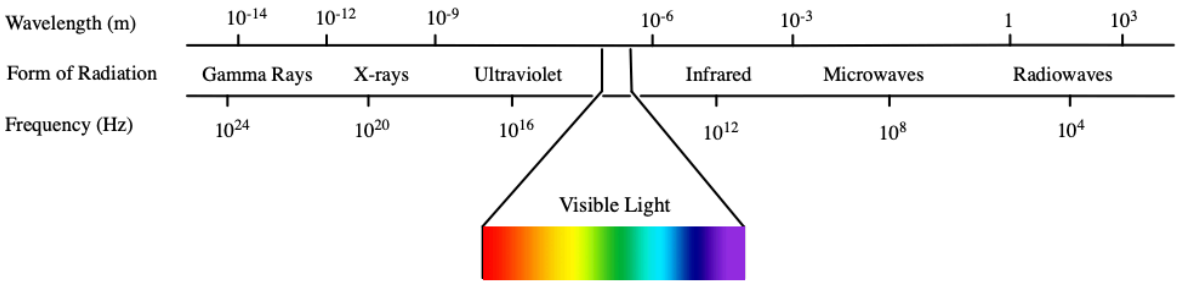

Figure 2.1 Electromagnetic Spectrum

All light waves can behave in a similar nature, as light is either scattered, reflected, absorbed, refracted, polarized, or diffracted.[23,24] Scattering of light occurs when light bounces off an object and travels in different directions.[23,24] An example of scattering is Rayleigh Scattering, which is responsible for the blue sky.[23,24] Reflection occurs when light comes in contact with an object and bounces off of it.[23,24] It is important to note that light that gets reflected is the color of an object, and all the other colors get absorbed.[23,24] Absorption refers to the phenomenon that occurs when light comes in contact with molecules and atoms, consequently causing

them to vibrate or undergo electronic excitation.[23,24] Moreover, if the wavelength of light matches the energy gap between the two levels, then it can be absorbed. This results in the promotion of electrons to excited states. When light waves come in contact with a different medium, or pass from one medium to another (if the two media have different indexes of refraction), they change directions.[23, 24] This is known as refraction. The diffraction of light occurs when light waves bend around an obstacle.[23, 24] Spectrometers often use diffraction of light by slits, gratings, or prisms to select a specific wavelength.[23,24]

There are four main transitions associated with different energetic degrees of freedom, namely: translational, rotational, vibrational, and electronic.[23] It takes more energy to transition between electronic energy levels than rotational and vibrational energy levels. Figure 2.2 illustrates the transitions between different energy levels. Vibrational energy levels and Stokes scattering are discussed in further detail in the following section.

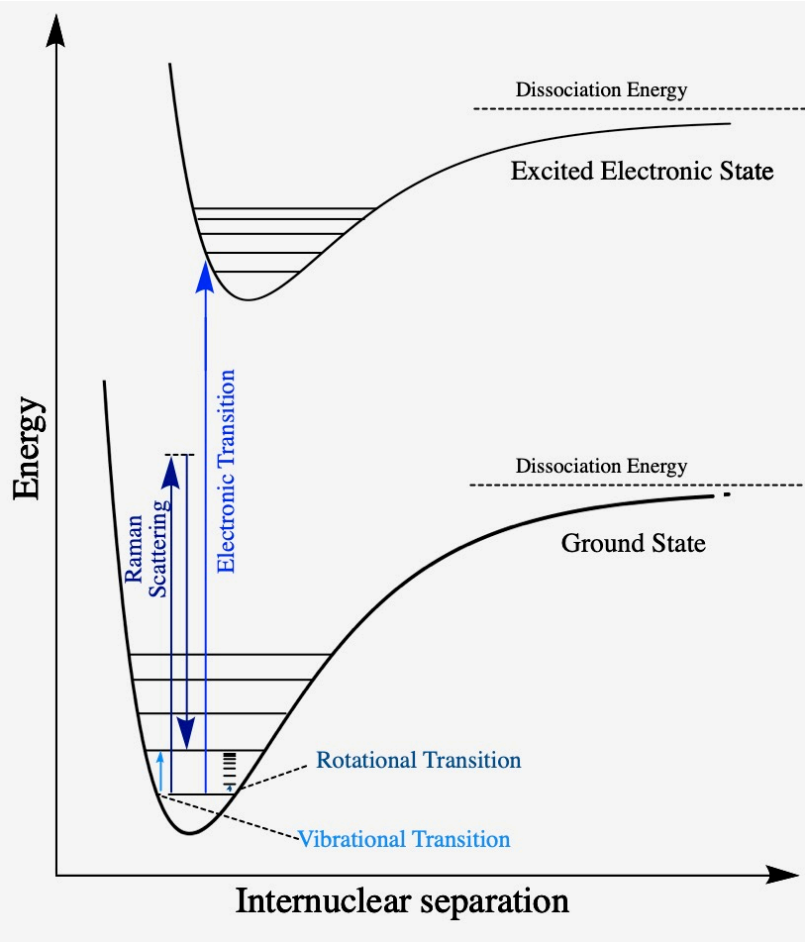

Figure 2.2 Types of different electromagnetic transitions.

2.2 Vibrational Spectroscopy

Molecular vibrations can be used to provide information about the physical properties of a compound, especially with regards to its structure and chemical bonds. When a molecule absorbs a photon, it gets excited to a higher energy state, causing a vibration to occur.[23,25,26] Selection rules serve to select which transitions

can actually take place.[23] The selection rule for vibrational transitions states that a transition is allowed if $\Delta v = \pm 1$, where v is the vibrational energy. However, overtone and combination bands do not follow $\Delta v = \pm 1$.

Molecular vibrations can be compared to the motions of a spring, which can be modeled using the harmonic oscillator.[23] Using this model, the two atoms are connected by a chemical bond, which is best represented by a spring.[23] The spring described by this model obeys Hooke's law.

$$F = -kx \tag{2.2}$$

In Equation 2.2, F is the force, k is the spring constant, and x is the displacement. The spring is at equilibrium when $x = 0$. Moreover, the potential energy (U_s) of this system can be described using Equation 2.3 In this equation ω represents the angular momentum.

$$U_s = \frac{1}{2} kx^2 = \frac{1}{2} k\omega^2 x^2 \tag{2.3}$$

Using the above equation, the quantum mechanical harmonic oscillator model can be obtained, in order to solve the Schrödinger equation (Eq. 2.5). The motion of the spring can be modeled as a longitudinal wave. The wavefunction can then be described using Equation 2.4.

$$\psi(x,t) = Ae^{i(kx-\omega t)} \tag{2.4}$$

$$\left[\frac{\hbar^2}{2\mathrm{m}}\frac{d^2}{dx^2}+\frac{1}{2}\mathrm{kx}^2\right]\psi(\mathrm{x}) \;=\; \mathrm{E}\psi(\mathrm{x}) \tag{2.5}$$

In this equation, m represents the mass, which can be replaced by μ, the reduced mass, if the masses are different. Moreover, $\hbar$ is equal to Planck's constant divided by 2π. Equation 2.6 represents the reduced mass, where m_1 and m_2 represent the masses of each atom in the molecule.

$$\mu = \frac{m_1 m_2}{m_1+m_2} \tag{2.6}$$

Consequently, the energy levels for a diatomic molecule can be represented by Equation 2.7. The energy levels are evenly spaced, regardless of the integer number of n, with the energy increasing linearly as n increases.[27]

$$\mathrm{E} = \; (\mathrm{n}+\frac{1}{2})\;\hbar\sqrt{\frac{\mathrm{k}}{\mu}} \tag{2.7}$$

The vibration of the molecular system can be determined using Equation 2.8, where v represents the frequency of vibration, k is the spring constant, and μ represents the reduced mass.

$$v = \frac{1}{2\pi}\sqrt{\frac{\mathrm{k}}{\mu}} \tag{2.8}$$

However, the energy of the photon is most commonly described by using the wavelength.[2,23] Another unit commonly employed is the wavenumber, $\tilde{v}$, which is

most often used when describing vibrational absorption of molecules.[2,23] The wavenumber is expressed in units of cm^{-1}, and can be found using Equation 2.9, where the sole difference between Equation 2.8 and Equation 2.9 is the inclusion of c, which is the speed of light.

$$\tilde{v} = \frac{1}{2\pi c}\sqrt{\frac{k}{\mu}} \tag{2.9}$$

In order to determine the vibrational modes of a molecule, it is important to describe the position of an atom. For a single atom, three coordinates–x, y, and z–can be used to describe its position.[28] However, for a molecule with N atoms, there are three normal modes that describe the translational motion of molecules. Consequently, the number of vibrational modes is equal to $3N-6$. For a linear molecule, the number of vibrational modes is equal to $3N-5$. This occurs because rotation around the linear axis does not alter the moment of inertia.[28,29] Moreover, a molecule can have different types of vibrational motions. Stretching motions include both symmetric and antisymmetric stretching, and bending motions include rocking, wagging, twisting, and scissoring motions.[23] Figure 2.3 illustrates the different types of vibrational motions for a molecule.

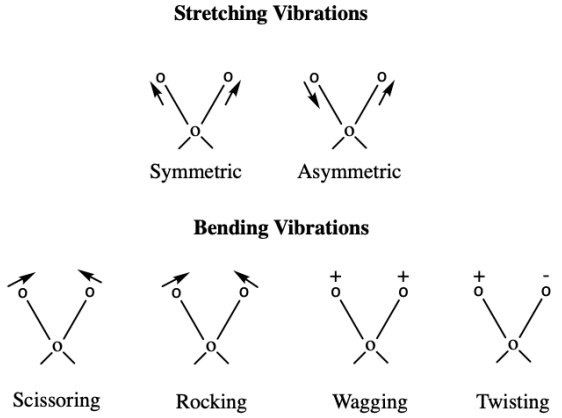

Figure 2.3 Stretching and bending vibrations for a molecule.

2.3 Raman Spectroscopy

In 1928, Sir C.V. Raman performed an experiment where he used light from a mercury lamp in order to analyze benzene, resulting in an unexpected scattering of light.[23] He observed its Raman spectrum, where the scattered light that emitted from the sample was different from the wavelength of the source.[23] This phenomenon was known as the Raman effect. Raman spectroscopy results from the inelastic scattering of photons resulting from an interaction with matter.[23] Raman spectroscopy is considered to be complementary to IR, as both techniques focus on elucidating the vibrational modes of a molecule.[23] For a molecule to be IR active it must undergo a net change in its dipole moment during its vibration.[23] In order for a molecule to be Raman active there must be a change in polarizability, in which the change in polarizability is asymmetric.[23] Consequently, certain vibrations

that are Raman active are not IR active and vice versa. It is possible, however, for a vibrational mode to be both IR and Raman active, or neither IR nor Raman active. Generally, symmetric vibrations are Raman active, whereas asymmetric vibrations and bending vibrational modes are IR active.[23] Most importantly, if a molecule has both IR and Raman signals that occur at the exact same frequency, then either the Raman peak or the IR peak is of greater intensity than its counterpart.[23] For molecules that are symmetrical about a central atom--such as carbon dioxide and benzene--both a Raman and IR active peak cannot co-exist at the same vibrational frequency because these molecules have a center of inversion.[23] This is known as the rule of mutual exclusion.[23]

Polarizability is defined by the ease by which a molecule will distort its electron cloud in response to an electric field.[23] Generally, larger molecules will have larger polarizability because of their increased number of electrons. Equation 2.9 shows the relationship between the induced dipole moment, μ_{ind}, polarizability, α, and the external electric field applied to a molecule.

$$\mu_{ind} = \alpha E \tag{2.9}$$

An electric field with a frequency of v_0 can be expressed using Equation 2.9, as light consists of oscillating magnetic and electric fields that are perpendicular to each other.[30,31]

$$E = E_0 \cos(2\pi v_0 t) \tag{2.10}$$

Since the polarizability of a molecule is impacted by the shape of the molecule and type of atoms, it can change as the molecule vibrates.[30-32] Consequently, the polarizability can be described using a Taylor Series expansion.[30-33]

$$\alpha = \alpha_0 + \left(\frac{\delta\alpha}{\delta r}\right)_{r_0} (r - r_0) \tag{2.11}$$

Conversely, the vibration of the molecule can be expressed using Equation 2.12.[30-33] Note that q_i can be used instead of r, as q_i is defined as a displacement coordinate, which corresponds to a change in radius that is dependent upon the normal mode.

$$q_i = q_i^0 \cos(2\pi \nu_i t) \tag{2.12}$$

Considering polarizability as resulting from a vibrational displacement rather than a change in radius results in the derivation of Equation 2.13.

$$\alpha = \alpha_0 + \left(\frac{\delta\alpha}{\delta q_i}\right)_0 q_i^0 \cos(2\pi v_i t) \tag{2.13}$$

Now, considering the original equation for the induced dipole moment, Equation 2.9 and Equation 2.10 can be substituted for E, and Equation 2.13 can be substituted in for α. These substitutions result in Equation 2.14.

$$\mu_{ind} = \alpha_0 E_0 \cos(2\pi v_0 t) + \left(\frac{\delta\alpha}{\delta q_i}\right)_0 E_0 \cos(2\pi v_0 t) q_i^0 \cos(2\pi v_i t) \tag{2.14}$$

In Equation 2.14 there is a multiplication of two different cosine terms. In order to solve for this, the trigonometric identity, shown in Equation 2.15 can be applied, consequently resulting in Equation 2.16. This represents a classical identity describing Raman scattering.[30-33]

$$\cos A \cos B = \frac{1}{2}[\cos(A + B) + \cos(A - B)] \quad (2.15)$$

$$\mu_{ind} = \alpha_0 E_0 \cos(2\pi v_0 t) + \frac{1}{2}\left(\frac{\delta\alpha}{\delta q_i}\right)_0 E_0 q_i^0 [\cos(2\pi(v_0 - v_i)t) + \cos(2\pi(v_0 + v_i)t)] \quad (2.16)$$

In Equation 2.16, the incident frequency is defined as v_0. This can be used to describe Rayleigh scattering. Stokes scattering is represented by $v_0 - v$, which symbolizes scattering that occurs at a lower vibrational frequency.[30-33] Lastly, anti-Stokes scattering is represented by $v_0 + v$, where scattering occurs at a higher vibrational frequency.[30-33]

As detailed in Equation 2.16, there are three different types of transitions that are associated with Raman spectroscopy: Rayleigh scattering, Stokes scattering, and anti-Stokes scattering. Figure 2.4 illustrates Rayleigh, Stokes, and anti-Stokes scattering.

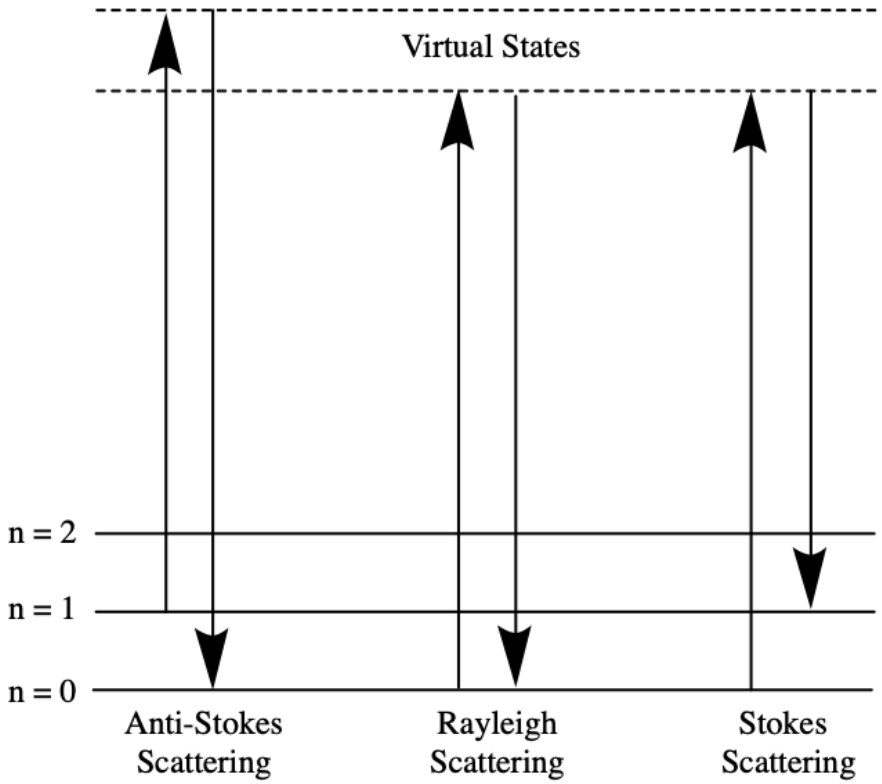

Figure 2.4 Rayleigh, anti-Stokes, and Stokes scattering.

Rayleigh scattering occurs when the energy of the scattered photon is the same as the emitted photon, meaning that if the photon is originally at the vibrational ground state and gets excited to a virtual state, the molecule will return to the vibrational ground state.[23] Consequently, Rayleigh scattering is known as an elastic process. On the other hand, both Stokes and anti-Stokes scattering are inelastic processes, and these are important for Raman scattering. Stokes scattering occurs when the energy of the emitted photon is less than the scattered photon. The photon will begin at the vibrational ground state, but following excitation it

will relax to a vibrational excited energy state. Anti-Stokes scattering starts at the vibrational excited state instead of starting at the vibrational ground state, and following excitation, the photon will relax to the vibrational ground state.[23] This results in the energy of the emitted photon being greater than the energy of the scattered photon.[23] Stokes lines are most commonly observed at room temperature. Anti-Stokes lines are extremely rare due to the prerequisite of the molecule being in a vibrational excited state, which is not typically seen at room temperature.[23]

CHAPTER 3

COMPUTATIONAL CHEMISTRY

3.1 The Schrödinger Equation

The primary goal of computational chemistry largely revolves around its capability to aid in the interpretation of physical measurements, predict the behavior of a system, and provide insight into the complex nature of a system.[34] Quantum mechanics provides the means by which to achieve these goals.[34] In quantum mechanics, particles exhibit wave-like properties, whose behavior can be elucidated by solving the Schrödinger Equation (Eq. 3.1).[35]

$$\hat{H}\psi = E\psi \tag{3.1}$$

The Schrödinger equation includes the Hamiltonian operator ($\hat{H}$), the wavefunction (ψ), and the total energy of the particle (E).[34] The Hamiltonian represents the sum of both the kinetic (T) and potential energies (V) in a system.[36] More specifically, the Hamiltonian accounts for the electron kinetic energy ($\hat{T}_e$), nuclear kinetic energy ($\hat{T}_n$), electron-nuclear attraction ($\hat{V}_{ne}$), electron-electron repulsion ($\hat{V}_{ee}$), and nuclear-nuclear repulsion ($\hat{V}_{nn}$).[36,37,38]

$$\hat{H} = \hat{T}_n + \hat{T}_e + \hat{V}_{nn} + \hat{V}_{ne} + \hat{V}_{ee} \tag{3.2}$$

However, the time-independent Schrödinger equation can only be solved for a one electron system.[37] Therefore, larger systems require using approximations in order to solve the equation.[37]

One of the approximations used is the Born-Oppenheimer approximation which assumes that electron and nuclear motions can be separated. Nuclei remain fixed in place relative to electrons due to the nuclei possessing a comparatively much larger mass.[36,37,38] Consequently, using Equation 3.2, $\hat{T}_n$ becomes zero and $\hat{V}_{nn}$ becomes a constant, since the nuclei are fixed in place. Equation 3.3 shows the electronic Hamiltonian equation, and Equation 3.4 shows the re-written electronic Schrödinger equation.[36,38]

$$\hat{H}_{elec}\psi_{elec} = E_{elec}\psi_{elec} \tag{3.3}$$

$$\hat{H}_{elec} = \hat{T}_e + \hat{V}_{ee} + \hat{V}_{ne} + \text{constant} \tag{3.4}$$

The second approximation involves the product of several single-electron wavefunctions. This is known as the Hartree product, which depends on both spatial and spin coordinates.[41]

$$\psi_{HP}(r_1, r_2, \ldots, r_N) = \phi_1(r_1)\phi_2(r_2)\ldots\phi_N(r_N) \tag{3.5}$$

The Hartree product (Eq. 3.5) gives us a symmetric wave function, so it does not fully describe the behavior of electrons since it does not account for spin.[39-

[41] This corresponds with the Pauli Exclusion Principle, which states that each electron must have different quantum numbers, and in order to occupy the same orbital, two electrons must have opposite spin values.[2] In order to satisfy these requirements, a Slater determinant for the new wavefunction can be constructed, where N represents the number of electrons, X_N represents spin states, and X_e represents the electrons.[39-41]

$$\psi = \frac{1}{\sqrt{N!}} \begin{bmatrix} \chi_1(x_1) & \chi_2(x_1) & \cdots & \chi_N(x_1) \\ \chi_1(x_2) & \chi_2(x_2) & & \chi_N(x_2) \\ & \vdots & \ddots & \vdots \\ \chi_1(x_e) & \chi_2(x_e) & \cdots & \chi_i(x_e) \end{bmatrix} \tag{3.6}$$

Most importantly, the determinant will change signs with the exchange of any two rows, and if two electrons occupy the same column (spin state), then the determinant will equal to zero.[41-43] The Hartree-Fock approximation aims to solve a multi-electron Schrödinger Equation by using a single Slater determinant consisting of the lowest energy combination of spin orbitals.[41,42] This involves creating Self-Consistent Field (SCF) equations and using another approximation, where the equations are rewritten as a linear combination of atomic orbitals (LCAO).[41,42]

Different electronic structure methods can be used in order to solve for the Schrödinger Equation. Semi-Empirical methods focus on simplifying the Hartree-

Fock approximation.[44] This method often results in quicker computing time, as it only considers valence electrons and uses approximations for one and two electron integrals.[44] Although this method can work relatively well for larger systems, it is often error prone.[44] On the other hand, *ab intio* methods aim to solve the time-independent Schrödinger Equation with great accuracy.[45] Consequently, this method can be quite expensive for larger systems.[45] Most methods also involve using basis sets. Basis sets are a set of functions used to define the orbitals.[42,46,47] There are several different types of basis sets that can be used, and it is important to take into account the nature of the system when choosing an appropriate basis set.

3.2 Computational Methods

Full geometry optimizations and corresponding harmonic frequency calculations were performed using common Density Functional Theory (DFT) methods. DFT methods are frequently used when investigating larger molecular systems due to their relative low-cost and accuracy.[43] These methods are based on the mathematical theorems proposed by mathematicians Pierre Hohenberg and Walter Khon.[48] They proposed theorems that related the ground state energy of the Schrödinger equation to electron density.[48,49] This in turn simplifies the system and

allows it to be more easily calculable, as the functional for electron density relies on an electron's x, y, and z coordinates.[43,48-50] In comparison to Hartree-Fock approximation methods, DFT methods attempt to account for the interaction of electrons in a system.[43,48-50]

Specifically the M06-2X[51] functional, and Dunning's aug-cc-pVDZ and aug-cc-pVTZ basis sets[52-54] were used for work included in Chapters 4 and 5. DFT methods have been previously used to study similar biomolecules,[55-60] with M06-2X specifically being shown to account for the dispersion that affects the hydrogen bonding interactions occurring in aqueous solvation shells due to long range electron correlation.[61-64] Lorentzian-type functions for each normal mode were combined in order to create the simulated Raman spectra.[65] Zero point energy (ZPE) corrections were applied for the comparison of relative energetics.

For both projects included in this work (Chapters 4 and 5), we collaborated with Professor David Magers (Mississippi College) for the computational work. Professor Magers performed full geometry optimizations and corresponding harmonic frequency calculations included in this thesis.

CHAPTER 4

NONCOVALENT INTERACTIONS BETWEEN TRIMETHYLAMINE N-OXIDE (TMAO), UREA, AND WATER

4.1 Abstract

Trimethylamine N-Oxide (TMAO) and urea are two important osmolytes with their main significance to the biophysical field being in how they uniquely interact with proteins. Urea is a strong protein destabilizing agent, whereas TMAO is known to counteract urea's deleterious effects. The exact mechanisms by which TMAO stabilizes and urea destabilizes folded proteins continue to be debated in the literature. Although recent evidence has suggested that urea binds directly to amino acid side chains to make protein folding less thermodynamically favored, it has also been suggested that urea acts indirectly to denature proteins by destabilizing the surrounding hydrogen bonding water networks. Here, we elucidate the molecular level mechanism of TMAO's unique ability to counteract urea's destabilizing nature by comparing Raman spectroscopic frequency shifts to the results of electronic structure calculations of micro-solvated molecular clusters. Experimental and computational data suggest that the addition of TMAO into an

aqueous solution of urea induces blue shifts in urea's HNH symmetric bending modes, which is evidence for direct interactions between the two co-solvents.

4.2 Introduction

Trimethylamine N-oxide (TMAO) and urea belong to an important class of small biomolecules called osmolytes. Osmolytes affect biological functionality through the regulation of water,[66-68] and many of the theories put forth to explain TMAO's ability to stabilize proteins and urea's denaturing effects have centered around their effective destabilization of hydrogen bonded networks of water.[55, 56, 69-96] Although most osmolytes are "compatible" and do not perturb macromolecules even at high concentrations, it is well known that urea is a protein destabilizer.[97] The study of the molecular-level mechanism for this destabilization has a long and storied history,[67, 71, 82, 98-105] and most recent studies agree that urea utilizes a direct mechanism to denature proteins.[101-106] For example, Wei et al. showed that urea directly interacts with the protein backbone to destabilize and unfold proteins.[107] However, a competing theory suggests that urea alters water structure and dynamics, thereby diminishing the hydrophobic effect and encouraging solvation of hydrophobic groups.[99] These water-urea interactions enhance hydrophobic groups' solvation in the unfolded state of proteins.

Contrary to the destabilizing effects of urea, it is well-established that TMAO stabilizes protein folding and counteracts the deleterious effects of urea.[108-110] The exact mechanism by which TMAO stabilizes protein folding is a popular topic of debate with some studies suggesting that solvent interactions do not play a large role in TMAO's stabilizing effects and therefore advocate direct stabilization.[111] More recent studies argue that TMAO counteracts denaturation primarily through strong solvent interactions or by an indirect effect.[55, 75, 84] It is known, for instance, that TMAO preferentially hydrogen bonds to three water molecules through its oxygen atom,[55, 56, 80] as shown in Figure 4.1 and that TMAO interactions make the hydrogen bonding network of water stronger than the network in pure water.[60, 73, 80] This so-called "iceberg water" in turn "dehydrates" the protein backbone carbonyl functional group, making the un-folded protein structure more unfavorable.[84] Previous studies have also found that TMAO is preferentially excluded from interacting with the protein backbone and side chains of proteins, leading to a destabilization of the unfolded structure.[112-114]

This hydrophobic effect places doubt on the possibility of TMAO directly interacting with proteins to counteract urea's destabilization of proteins. This exclusion from backbone interaction, coupled with the fact that TMAO molecules

take up space around the proteins, suggests that there is likely another mechanism by which TMAO affects protein stability in the presence of urea.

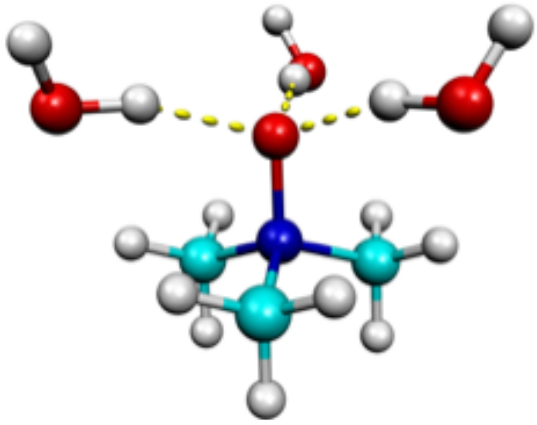

Figure 4.1 TMAO is known to preferentially hydrogen bond to three water molecules through its oxygen atom.[55, 56, 80]

When both osmolytes are together in solution, TMAO counteracts urea's destabilizing effects on proteins. In fact, it has been shown that TMAO can effectively counteract urea's denaturation of proteins in concentration ratios as low as 1:2 TMAO to urea.[99, 115, 116] This counteraction is maximized when the osmolytes are in a 2:1 TMAO to urea ratio.[117] The molecular level mechanism by which this counteraction occurs is still unclear, although it has become a very popular topic for study in recent years.[77-80, 85, 86, 88, 89, 91, 93, 118] One popular hypothesis is that that TMAO's stabilization of the folded protein overpowers the stabilization of the

unfolded protein state by urea.[108, 115, 116] Although favorable TMAO interactions with protein side-chains actually promote protein denaturation, the highly unfavorable TMAO peptide-backbone interactions offset the favorable TMAO side-chain interactions. Urea, on the other hand, interacts favorably with both the protein peptide backbone and protein side chains. Because side chain interactions for both TMAO and urea favor the unfolded state, TMAO exclusion from the backbone could be the sole origin of protein protection. This mechanism would also account for TMAO's ability to counteract urea in all proteins, regardless of the side chains.[83]

Although much research has focused on how TMAO and urea interact independently or collectively with proteins, until very recently, few studies have focused on the molecular-level interactions between the two osmolytes themselves. In a neutron diffraction study, Meerman et al. suggested that the oxygen atom on TMAO preferentially interacts with the amine groups of urea rather than with water when both osmolytes are together in solution.[80] This direct TMAO-urea interaction, coupled with TMAO's exclusion effects, would account for the ability of TMAO to counteract urea denaturation in solutions of 1:2 TMAO-urea concentration ratio. This hypothesis has recently been supported by Ganguly, et al. who showed using theoretical models that there is a delicate balance of TMAO-

water, TMAO-TMAO, and TMAO-urea interactions.[89] Sahle, et al. studied the structure of water in concentrated TMAO-urea solutions using inelastic X-ray scattering and concluded that the hydrogen bonding structure of water remains intact if both osmolytes are present in low concentrations and that TMAO and water interact much more strongly than urea and water.[119]

We seek here to elucidate the effects of molecular level interactions of TMAO and urea in solution using a combination of Raman vibrational spectroscopy and the results of electronic structure calculations. We, and others, have shown previously that shifts in vibrational frequencies can indicate hydrogen bonding in amphoteric molecules, with red-shifting occurring when the amphoteric species acts as a proton donor and a blue shift occurring when the amphoteric species acts as a proton acceptor.[51, 52, 57-59, 120-122] These shifts are helpful in revealing the structure of water around TMAO and urea. In our previous studies, we used Raman spectra and the results of electronic structure calculations to elucidate the structure of water, methanol, ethanol, and ethylene glycol in solution with TMAO.[51, 52] Here, we use the subtle changes in Raman spectra that result from TMAO/urea inter-actions to paint a molecular-level picture.

4.3 Spectroscopic Methods

Commercial grade anhydrous trimethylamine N-oxide (Tokyo Chemical Industry) and urea (Sigma-Aldrich) were used without further purification. The excitation sources employed for Raman spectroscopy were the 532 nm line from a Horiba LabRAM HR Evolution Raman spectrometer with an 1800 grooves/mm grating. Raman Spectra of saturated TMAO in water ($\chi_{\mathrm{TMAO}} = 0.08$, 5 M), saturated urea in water ($\chi_{\mathrm{UREA}} = 0.27$, 20 M), and a 1:1 mixture of these solutions were collected. The concentrations of urea and TMAO in this mixed solution was 10 M and 2.5 M, respectively, leading to a ratio of four urea molecules to every one TMAO molecule. These concentrations were selected to maximize the number of osmolyte molecules in solution. Additional mixtures at lower concentrations were created to explore the effect of changing this ratio.

4.4 Theoretical Methods

Optimized equilibrium geometries and corresponding electronic energies of TMAO, urea, and TMAO and urea interacting with up to four water molecules were obtained using density functional theory.[52, 53, 123] Truhlar's Minnesota functional M06-2X was utilized.[51] The basis sets used are the augmented correlation consistent basis sets aug-cc-pVDZ and aug-cc-pVTZ created by Dunning and co-workers.[124]

All calculations were performed using the Gaussian09 software.[125] Simulated Raman spectra were created by summing Lorentzian profiles for each normal mode.[65]

4.5 Spectroscopic Results

Figure 4.2 compares the Raman spectra of saturated aqueous solutions of TMAO and urea to that of a 1:1 mixture of these solutions. This concentration was chosen to maximize the number of osmolytes present in solution. We showed previously that increasing dilution does not affect features in the Raman spectra of TMAO.[51, 52] At first glance the spectra are additive.[65] However, when comparing the locations of nor-mal modes for TMAO and urea in the three solutions, there is a noticeable 11 cm^{-1} blue shift in the broad feature centered at 1591 cm^{-1}. Figure 4.3 highlights this spectral region in greater detail. Spectra of additional concentrations were collected to explore the effects of con-centration and molecular ratio. In Figures 4.2 and 4.3, there are four urea molecules for every TMAO molecule. Figure 4.4 compares the Raman spectrum of a 4 M aqueous urea solution to that of an aqueous solution that is 4 M urea and 4 M TMAO (1:1 molecular ratio). This yields a result nearly identical to that shown in Figure 4.3.

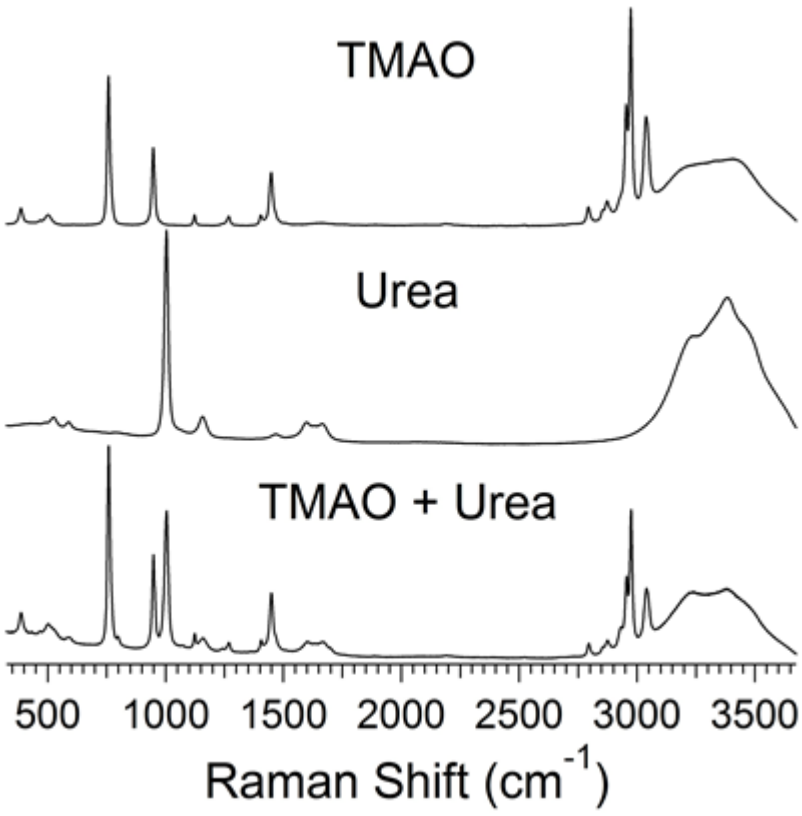

Figure 4.2 Raman Spectra of saturated aqueous TMAO (top) and urea (middle) solutions and mixture of these saturated solutions.

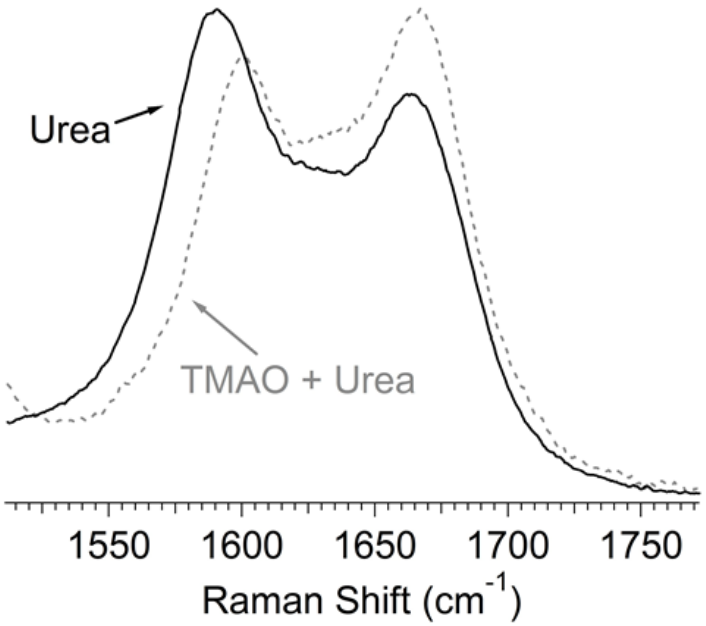

Figure 4.3 Experimental Raman spectra in the region of urea's HNH bending motions of a saturated urea solution (solid) and a urea:TMAO solution (dashed) created by combining a saturated urea solution with a saturated TMAO solution.

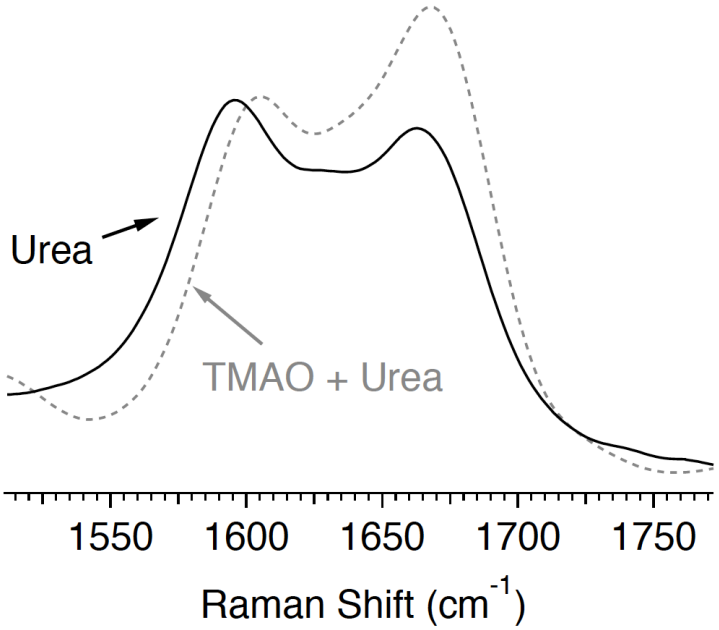

Figure 4.4 Raman spectra of 4 M aqueous urea compared to an aqueous solution that is 4 M urea and 4 M TMAO.

4.6 Theoretical Results

To aid in the analysis of experimental Raman spectral results, simulated Raman spectra were created using optimized structures of molecular clusters obtained using electronic structure theory. It is important to point out that since we are comparing aqueous solutions of TMAO and urea, the study of hydrated molecular clusters is essential. Figure 4.5 shows the minimum energy structures of TMAO interacting with urea and water. Hydrated urea structures are also shown in Figure 4.5 since we wish to elucidate the effect of introducing TMAO into hydrated urea. The relative energies for these different structures are presented in Table 4.1.

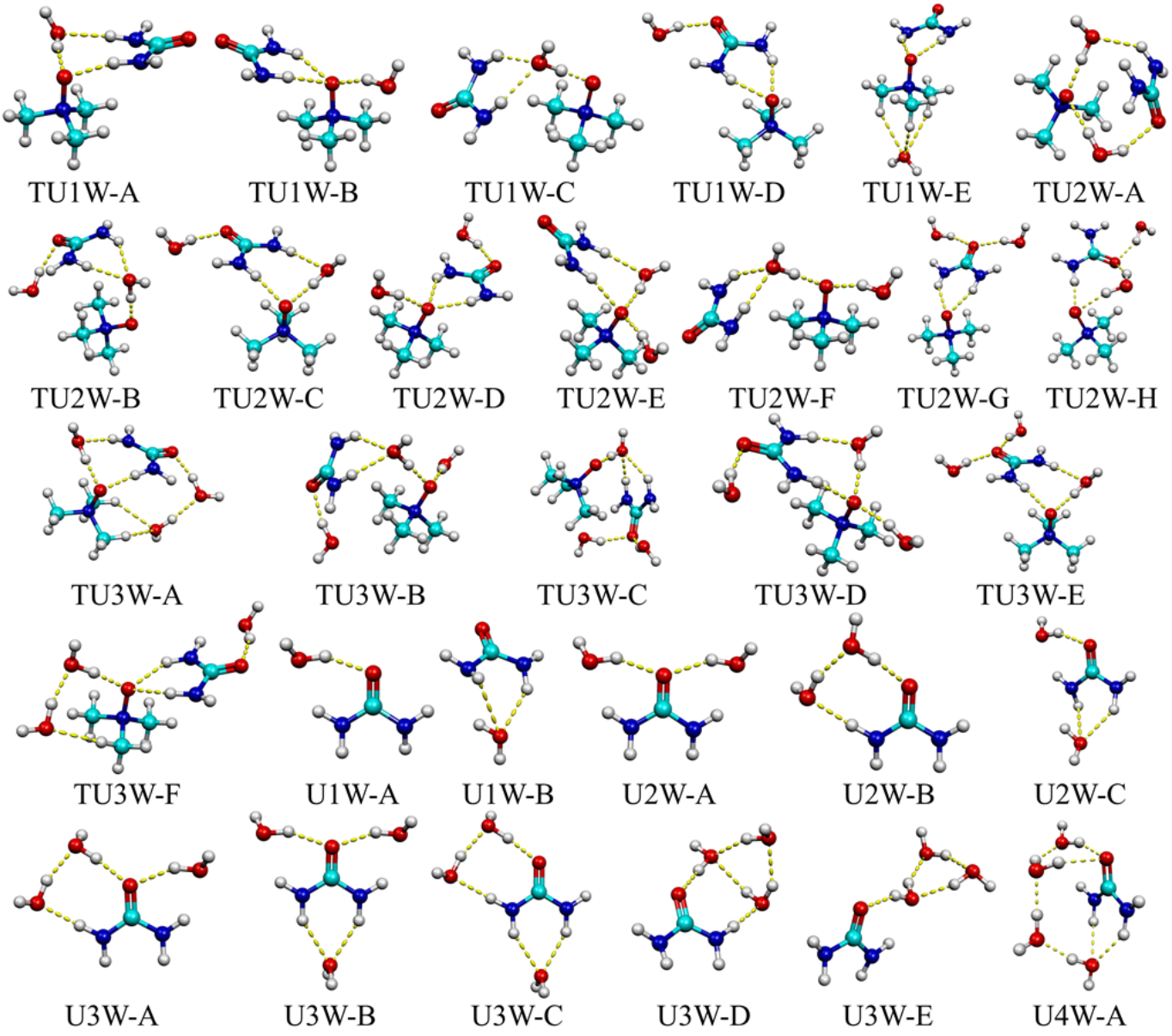

Figure 4.5 Optimized structures of TMAO, urea, with up to four water molecules.

Minimum Energy Structures	Relative Energies (kcal/mol)	
	aug-cc-pVDZ	aug cc-pVTZ
TMAO-Urea-1 Water		
TU_1W-A	0.00	0.00
TU_1W-B	0.88	0.74
TU_1W-C	0.96	0.75
TU_1W-D	1.38	1.04
TU_1W-E	7.26	6.95
TMAO-Urea-2 Waters		
TU_2W-A	0.00	0.00
TU_2W-B	0.33	0.20
TU_2W-C	0.64	0.65
TU_2W-D	1.40	1.17
TU_2W-E	1.22	1.67
TU_2W-F	1.59	1.94
TU_2W-G	2.66	2.44
TU_2W-H	2.97	2.93
TMAO-Urea-3 Waters		
TU_3W-A	0.00	0.00
TU_3W-B	0.71	0.98
TU_3W-C	1.06	1.29
TU_3W-D	1.43	1.69
TU_3W-E	2.44	1.86
TU_3W-F	3.07	3.04
Urea-1 Water		
U_1W-A	0.00	0.00
U_1W-B	3.04	3.16
Urea-2 Waters		
U_2W-A	0.00	0.00
U_2W-B	0.27	0.23
U_2W-C	2.69	2.93
Urea-3 Waters		
U_3W-A	0.00	0.00
U_3W-B	1.03	1.13
U_3W-C	2.22	2.39
U_3W-D	2.21	2.46
U_3W-E	3.98	3.84

Table 4.1 Relative energies in kcal/mol of the minimum energy TMAO/Urea/Water structures using the M06-2X method and either aug-cc-pVDZ or aug-cc-pVTZ basis sets (including ZPE corrections).

We previously reported optimized molecular clusters involving TMAO and water and demonstrated that TMAO's oxygen atom played a critical role in directing the hydrogen bonded solvent networks. [51, 52] Zero-point energy corrections were performed on all structures. For the lowest energy conformations involving both TMAO and urea, a water molecule is found between the oxygen atom of TMAO and a hydrogen atom on one nitrogen atom of urea. For the conformations involving only urea, the lowest energy conformations have water molecules oriented around urea's oxygen atom. Interestingly, one of the conformations (U3W-E) which exhibits an intact hydrogen bond network is significantly higher in energy than conformations with disrupted networks.

Vibrational frequencies and Raman activities were calculated and Raman spectra were simulated by summing Lorentzian profiles of each normal mode. Figure 4.6 compares the simulated Raman spectrum for the lowest energy conformation of hydrated urea (U3W-A) with the lowest energy structure involving TMAO, urea, and three water molecules (TU3W-A) in the region of urea's H-N-H bending motions using two different Lorentzian peak widths. M06-2X/aug-cc-pVTZ frequencies have been scaled by 0.97 to partially correct for anharmonicity. The simulated spectrum constructed with the experimentally observed Lorentzian

peak width is remarkably similar to the experimental spectrum and results from seven overlapped normal modes. An overall blue shift of 9 cm^{-1} of the large feature centered 1575 cm-1 is reproduced by theory and agrees very well with the 11 cm^{-1} shift observed experimentally.

The spectra with narrow peak widths are included to show the contributions from that yield the broad experimentally observed features.

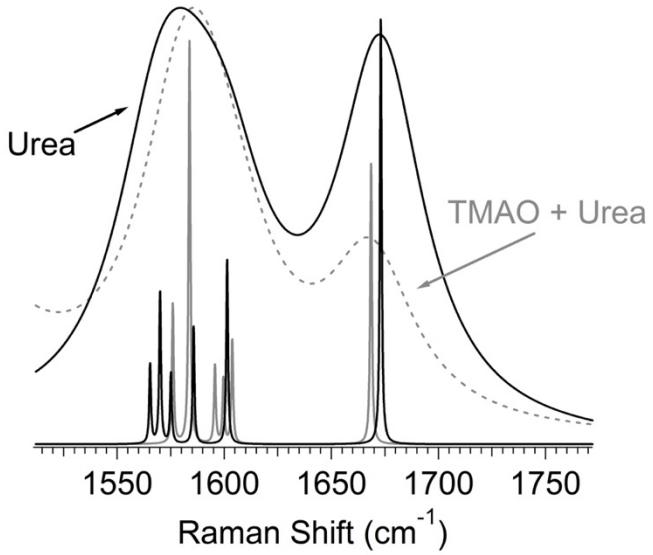

Figure 4.6 Simulated Raman spectra of TU3W-A compared to U3W-A.

The very good agreement between experiment and theory suggests that the theoretical simulations can be used to assign the experimental features. The most hydrated optimized structure is likely to be the most accurate simulation of saturated experimental solutions.[57] In this case, this is the dimer with three water

molecules (TU3W-A). Upon examination of the individual normal mode trajectories, the peak in the experimental urea spectrum at 1591 cm^{-1} in Figure 4.3 that experiences the blue shift in the presence of TMAO is dominated by the H-N-H symmetric bending mode of urea. Most other hydrated structures also show this same blue shift, suggesting that interactions between urea and TMAO likely involve urea's N-H bonds.

In addition to the lowest-energy case presented above, a comparison of U3W-B with TU2W-G also yields strong evidence for this direct interaction. When comparing the structures of U3W-B with TU2W-G, two water molecules are hydrogen bonded to urea's oxygen atom. In U3W-B, the lower hydrogen atoms on each NH2 group of urea is hydrogen bonded to the oxygen atom of another water molecule. In TU2W-G, this third water is directly replaced by a TMAO molecule with the same number of hydrogen bonds. In U3W-B, the mode that has the highest degree of HNH symmetric bend is 1611 cm^{-1} while this is blue-shifted in TU2W-G to 1633 cm^{-1}. More evidence comes from a comparison of TU3W-A with U4W-A. The number of hydrogen bonds to urea are the same in each structure. In U4W-A, the HNH symmetric bend is 1637 cm^{-1} compared to 1642 cm^{-1}, showing again that replacing a water molecule with TMAO directly leads to a blue shift. Another good example of this effect is the replacement of the water molecule in

U3W-A which is hydrogen bonded to the hydrogen atom in urea with a TMAO molecule (TU2W-H). In U3W-A, the HNH symmetric bend is 1635 cm^{-1} and the HNH symmetric bend in TU2W-H is 1637 cm^{-1}. This is the smallest blue shift, likely because only one of the hydrogen atoms in urea is involved in a hydrogen bond in both of these structures. Thus, one would expect the blue shift to be smaller in this last comparison.

The solvation of urea has been studied previously by others and provides insight into urea's favorable interaction sites.[126-132] Water molecules tend to aggregate to either side of the carbonyl oxygen on urea and in between the two amine groups of urea. The lower energy conformations of urea and water split the water molecules be-tween multiple interaction spots. Interestingly, water molecules do not maintain a hydrogen bond network in the presence of both urea and TMAO. This is in stark contrast to our earlier observations for pyrimidine and water interactions.[57, 58] This is also in contrast to TMAO-water structures in which waters prefer to interact with each other in the lower energy structures.[56] These findings support the literature case that urea de-stabilizes water hydrogen bonding networks, allowing water molecules to attack protein structures.[84] In the lower energy conformations of the dimer with water, the blue shift found experimentally is reproduced computationally when the TMAO molecule's oxygen acts as a

hydrogen bond acceptor and the amine hydrogen atoms act as hydrogen bond donors. In these structures, the oxygen atom on TMAO interacts with one of the hydrogen atoms on a nitrogen atom of urea and one water molecule. This data suggests that TMAO directly interacts with urea at high concentrations, in agreement with studies by Meersman, et al.[80, 85] This contrasts other studies that suggest that no such interaction is present at physiological concentrations.[85, 91, 119, 133]

4.7 Conclusions

The interactions between TMAO and urea in saturated aqueous solutions were investigated using Raman spectroscopy and electronic structure computations. Very good agreement between experiment and theory suggests urea and TMAO directly interact in aqueous solution, at least at high concentrations. Molecular cluster conformations with central urea molecules are lower in energy than those that maintain a hydrogen-bonded water network. When TMAO is introduced to urea in aqueous solution, a significant blue shift in the H-N-H symmetric bending mode of urea is observed experimentally. This result is observed both in conformations of TMAO and urea with water and in conformations with-out water, suggesting the blue shift directly results from interactions between TMAO and

urea. Together, these results suggest that, at least at high concentrations, TMAO directly counteracts urea's destabilizing effect on proteins through direct interactions with urea's amine groups.

4.8 Note

This work was published in the *Journal of Physical Chemistry B*, and it was featured as a cover for the September 27, 2018 issue.[134] Professor David Magers, Sarah G. Zetterholm, Leeann Boutwell, Johnathan Bethea, and Professor Shelley A. Smith (Mississippi College) performed full geometry optimizations and corresponding harmonic frequency calculations included in this thesis. I then used that data to create simulated spectra.

Figure 4.7 *Journal of Physical Chemistry B*, September 27, 2018 issue.

CHAPTER 5

RAMAN SPECTROSCOPIC AND QUANTUM CHEMICAL INVESTIGATION OF THE EFFECTS OF TRI-METHYLAMNINE N-OXIDE (TMAO) ON HYDRATED GUANIDINIUM AND HYDROGEN BONDED WATER NETWORKS

5.1 Abstract

The effects of trimethylamine-N oxide (TMAO) on guanidinium chloride and hydrogen-bonded networks of water are explored in this joint Raman spectroscopic and quantum chemical study. Both TMAO and guanidinium are osmolytes that affect the stability of proteins, as TMAO is known to stabilize and counteract the destabilizing effects of guanidinium. While guanidinium is very similar in chemical structure to urea, the exact mechanisms of the molecular interactions between guanidinium, TMAO, and proteins continue to be investigated. Herein, we use Raman spectroscopy to elucidate the physical interactions between TMAO and guanidinium in aqueous solutions to better understand how these important osmolytes interact with each other and affect adjacent hydrogen-bonding networks of water. Comparing experiment to theory yields good agreement, and allows for

the identification and tracking of different vibrational modes. It was determined that adding TMAO into an aqueous solution of guanidinium induces a blue shift (shift to higher energy) in guanidinium's H-N-H bending modes, which is indicative of direct interactions between the two osmolytes and similar to the earlier results observed for TMAO interacting with urea.

5.2 Introduction

Osmolytes belong to a class of small organic molecules that play crucial roles in protecting organisms' cells against environmental stressors, such as high pressure, salinity, and temperature.[67, 68, 135, 136] Such environmental stressors induce osmotic changes in cells, which in turn can negatively impact proteins and disrupt important physiological processes.[137] Several aquatic organisms such as coelacanth (sharks) and marine elasmobranchs (rays) naturally possess elevated levels of osmolytes in their tissues to help combat environmental stressors.[115, 138, 139] Osmolytes are typically categorized into three classes: amino acids and their derivatives, polyhydric alcohols, and methylamines.[138, 140, 141] While osmolytes of the first two classes have little effect on protein function, those of the third class are known to counteract the negative effects of urea and guanidinium chloride.[68, 138, 142]

Osmolytes favor protein stability and have the potential to induce the folding of proteins *in vitro*.[97, 143, 144] Trimethylamine N-oxide (TMAO) is a well-known member of this class of osmolytes.[97] TMAO counteracts the denaturing effects of urea and guanidinium chloride on proteins and induces the folding of proteins at pH values above its pKa of 4.7.[80, 138, 145] Guanidinium chloride, a guanidinium salt, is found in urine as a by-product of protein metabolism and has a denaturing effect on proteins, similar to urea.[146] Figure 5.1 shows the structures of TMAO, urea, and the guanidinium cation.

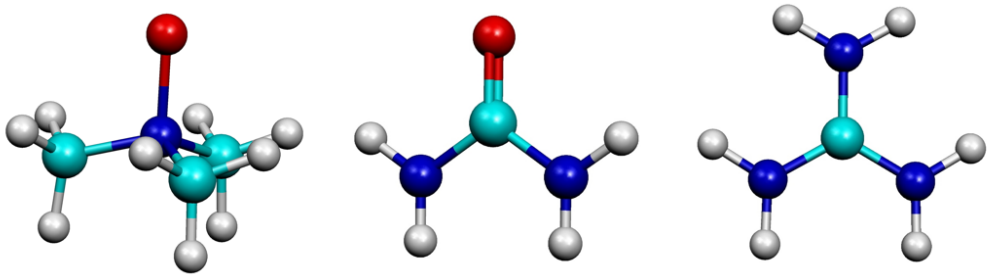

Figure 5.1 Molecular structures of TMAO (left), urea (middle), and guanidinium (right).

While guanidinium is structurally similar to urea having two amine groups, the exact mechanism by which guanidinium destabilizes proteins is largely unknown.[147-151] Moreover, there has been a great deal of controversy surrounding the molecular interactions between denaturants such as guanidinium and

stabilizing osmolytes such as TMAO. One popular theory suggests that the stabilization of proteins is mediated through the direct interaction between the osmolyte and the protein,[143, 152, 153] which is commonly known as the "direct effect."[55, 83, 107, 110, 154, 155] Conversely, other studies have concentrated on the effects that the osmolyte has on hydrogen-bonded water networks, which has been shown to affect the stability of the protein through the rearrangement of the solvation shell.[144, 156, 157] This theory is known as the 'indirect effect."[51, 158-160] TMAO's indirect interaction with the amide unit on peptide backbones is thought to play a significant role in protein stabilization.[76, 144, 161] This indirect interaction between TMAO and the protein's functional groups has an impact on water's structure through an increase in both the number of water-water hydrogen bonds and the strength of these bonds.[76, 162] Previous studies by us and others have shown that TMAO forms hydrogen bonds with an average of three water molecules, and that the water network does not interact with the methyl groups due to their hydrophobic nature, which creates a void.[55, 56, 80, 144] This void space causes the surrounding water molecules to become "ice-like" by creating a stronger hydrogen bonding network, a phenomenon known as the "hydrophobic effect" with the formation of "iceberg water."[55, 144, 156, 157, 163, 164] The occurrence of the hydrophobic effect, along with TMAO's indirect interactions with the amide unit on the peptide

backbone, suggests that TMAO does not have to directly interact with proteins to counteract the deleterious effects of guanidinium.[144]

When both TMAO and guanidinium are present together in solution, TMAO is known to counteract the destabilizing effects of guanidinium. Unlike urea, the charged guanidinium cation does not destabilize proteins by hydrogen bonding to the peptide group in proteins.[151] A number of molecular dynamics studies have investigated the mechanisms governing interactions between guanidinium and proteins. These studies have suggested that guanidinium interacts with proteins through electrostatic interaction with polar or charged side chains,[165-167] by hydrogen bonding with the carboxylic acid groups,[151] hydrophobic interactions between the cation (Gdm+) and aromatic groups, [162,168] or by disrupting the structure of surrounding water molecules.[169, 170] Guanidinium's ability to readily form a hydrogen bond with water within the plane of the ion suggests that this effect may aid in its ability to denature proteins,[163, 166, 171-173] supporting the idea that guanidinium indirectly interacts with the protein. While much research has focused on TMAO's interactions with water, few studies have examined molecular level interactions between guanidinium and water. One exceptions is a gas-phase study by Cooper et al. that explored the hydration of guanidinium using laser-based infrared spectroscopy.[166]

Since the two denaturants urea and guanidinium[80] are similar in chemical structure, it is beneficial to take into account previous work describing the interactions between TMAO and urea when considering guanidinium. One previous study on TMAO-urea interactions by Meersman et al. suggested that TMAO has the ability to counteract urea's denaturation of proteins in solutions at a concentration ratio of 1:2 TMAO: Urea.[80, 93, 99, 115, 116] Moreover, TMAO's ability to counteract urea is increased in solutions of a 2:1 TMAO: urea concentration ratio.[108, 115, 116] Meersman suggested that this phenomenon is largely due to the oxygen atom of TMAO interacting with the amine groups of urea instead of hydrogen bonding with neighboring water molecules; however, the result of this paper was later revised, with Meersman reporting weak noncovalent interactions between the osmolytes.[80, 85] On the other hand, other studies have suggested that TMAO and urea interact via hydrogen bonding, which prevents urea from interacting with the proteins.[85, 101, 102] Some results intimated that TMAO strengthens the tetrahedral conformation of the surrounding water molecules while urea weakens them, suggesting a stronger interaction between TMAO and water compared to urea and water.[85, 112, 174-176] More recently, we showed that TMAO preferentially interacts with urea, which induces a blue shift (shift to higher energy) in the vibrational frequencies of the H-N-H symmetric bending mode of urea.[80, 134]

Here, we examine the Raman spectra of mixtures of TMAO and guanidinium in aqueous solutions and compare our results to theoretical predictions in order to gain a better understanding of the relevant interactions between the two osmolytes. Based on previous work, the structural similarities between guanidinium and urea suggests that TMAO should have the ability to counteract guanidinium's denaturation of proteins in solutions with as little as a 1:2 TMAO to guanidinium concentration ratio. Few studies, however, have focused on elucidating TMAO's ability to counteract guanidinium's denaturation of proteins at different concentration ratios. Although guanidinium may elicit a different effect on proteins than urea, it should induce a similar change in the surrounding hydrogen bonded water network.[169]

5.3 Experimental Methods

Commercial grade anhydrous trimethylamine N-oxide (Sigma Aldrich) and an 8M solution of Guanidinium-Chloride (Sigma Aldrich) were used without further purification. A Horiba LabRAM HR Evolution Raman Spectrometer with CCD camera detection was used. The excitation source used for Raman spectroscopy was the 532nm line of a diode laser with either a 600 or 1800 grooves/mm grating. Spectra were obtained for saturated TMAO in water (χ_{TMAO}= 0.27, 8M) and Gdn-

HCl in water ($\chi_{\text{Gdn-HCl}} = 0.38$, 8M). TMAO:Gdn-HCl ternary solutions at 1:1 (4M:4M) and 1:2 (2M:4M) molar concentration ratios were then created from these and studied.

5.4 Theoretical Methods

Full geometry optimizations and corresponding harmonic frequency calculations were performed on TMAO, guanidinium cation, and water using common DFT methods, specifically the M06-2X[51] and ωB97XD[177] functionals, and using Dunning's aug-cc-pVDZ and aug-cc-pVTZ basis sets.[52-54] DFT methods have been previously used to study similar biomolecules,[55-60, 178] with M06-2X specifically being shown to account for the dispersion that affects the hydrogen bonding interactions occurring in aqueous solvation shells.[61-64] Lorentzian-type functions for each normal mode were combined in order to create simulated Raman spectra.[65, 134] Zero point energy (ZPE) corrections were applied for the comparison of relative energetics

5.5 Spectroscopic Results

The Raman spectra of neat aqueous solutions of either guanidinium or TMAO of various concentrations were analyzed first to confirm that spectral features of each

did not vary with concentration. Figure 5.2 compares the Raman spectra of 8M TMAO and 8M guanidinium solutions to that of an equimolar (4M:4M) TMAO: guanidinium solution. For the vast majority of spectral features, no changes are obvious for either TMAO or guanidinium in the 1:1 mixture. However, two apparent blue shifts are observed in the region of guanidinium's H-N-H bending modes, as highlighted in Figure 5.3.

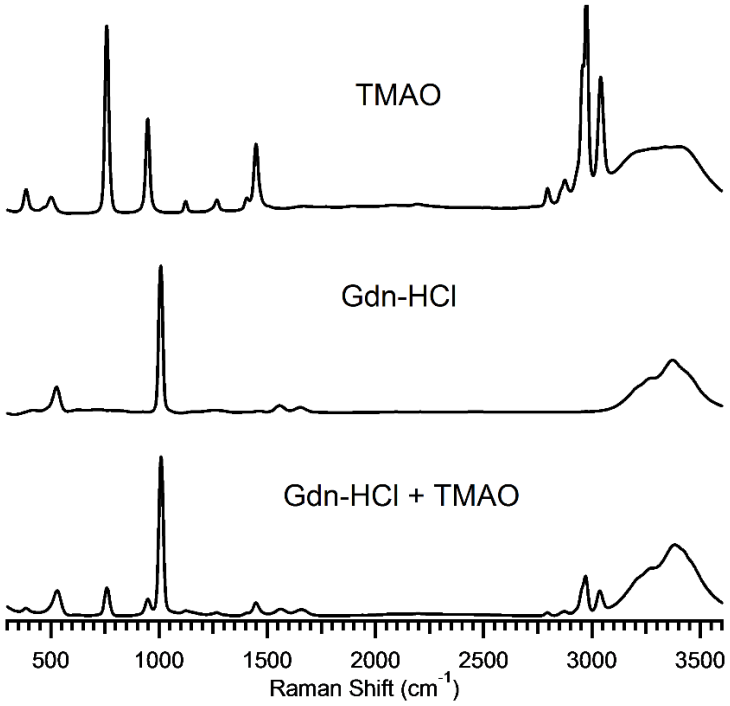

Figure 5.2 Raman spectra of saturated aqueous TMAO (top, 8M) and guanidinium (middle, 8M) solutions compared to a mixture of these saturated solutions (4M:4M).

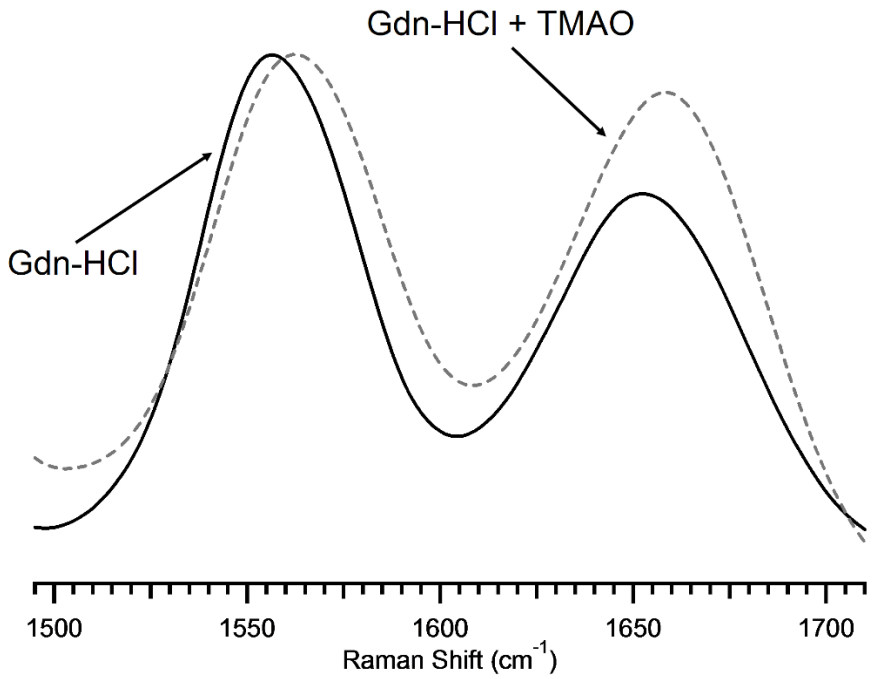

Figure 5.3 Experimental Raman spectra in the region of guanidinium's H-N-H bending motions of a saturated guanidinium solution (solid) and a saturated guanidinium-TMAO solution (dashed).

The first change is a 6.6 cm^{-1} blue shift in the first broad feature located at 1556.5 cm^{-1} and the second is an 8.6 cm^{-1} blue shift in the second peak of the broad feature located at 1652.0 cm^{-1}. We previously reported that shifts in vibrational frequencies can serve as indicators for the formation of hydrogen bonds.[55, 56, 83, 122, 179] More specifically, blue shifting is represented by an increase in vibrational frequency, and is indicative of the amphoteric species acting as a proton acceptor.[55-59, 120, 122] In addition to comparing the Raman spectra of equimolar concentrations of ternary TMAO: guanidinium solutions, a 1:2 (2M:4M) solution of TMAO:

guanidinium was also examined and the result is shown in Figure 5.4. Even in solutions where molecular concentrations of guanidinium are double that of TMAO, both broad features still undergo a blue shift. The feature at 1556.5 cm^{-1} undergoes a 5.9 cm^{-1} shift to 1562.4 cm^{-1}, and the second exhibits a 7.2 cm^{-1} shift. The noticeable changes in both broad features suggest an interaction between TMAO and guanidinium and stronger interactions between TMAO and water in comparison to guanidinium and water.

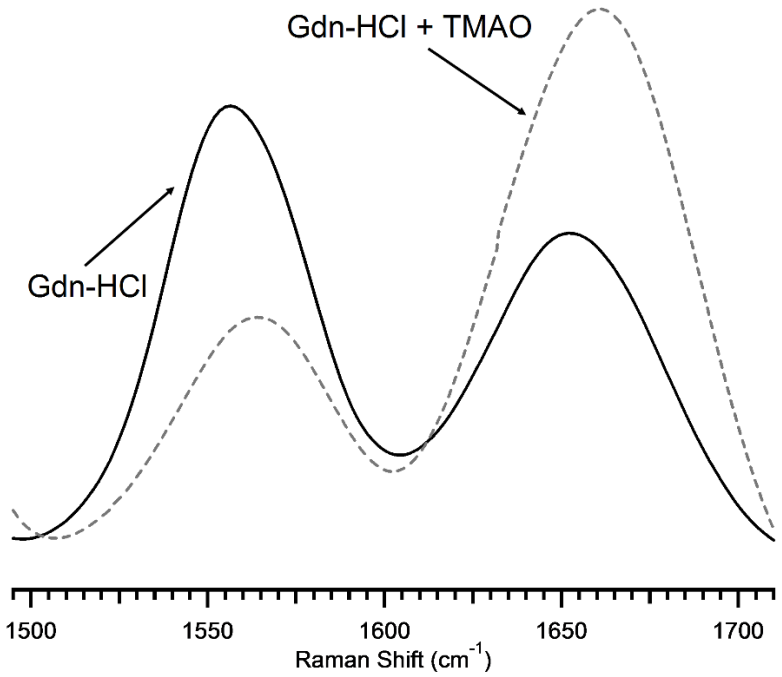

Figure 5.4 Experimental Raman spectra in the region of guanidinium's H-N-H bending motions of a saturated guanidinium solution (solid) to a 1:2 TMAO-guanidinium solution (dashed).

5.6 Theoretical Results

In order to characterize the individual vibrational motions occurring at each peak in the experimental Raman spectra, quantum chemical approximation methods were employed to generate simulated Raman spectra for the systems of interest. Shown in Figure 5.5 are the optimized molecular geometries of TMAO/guanidinium/water and guanidinium/water molecular clusters. The relative energies for each of the hydrated structures were calculated and are included in Table 5.1. Zero point energy corrections were performed on all molecular structures and are included in the presented energies.

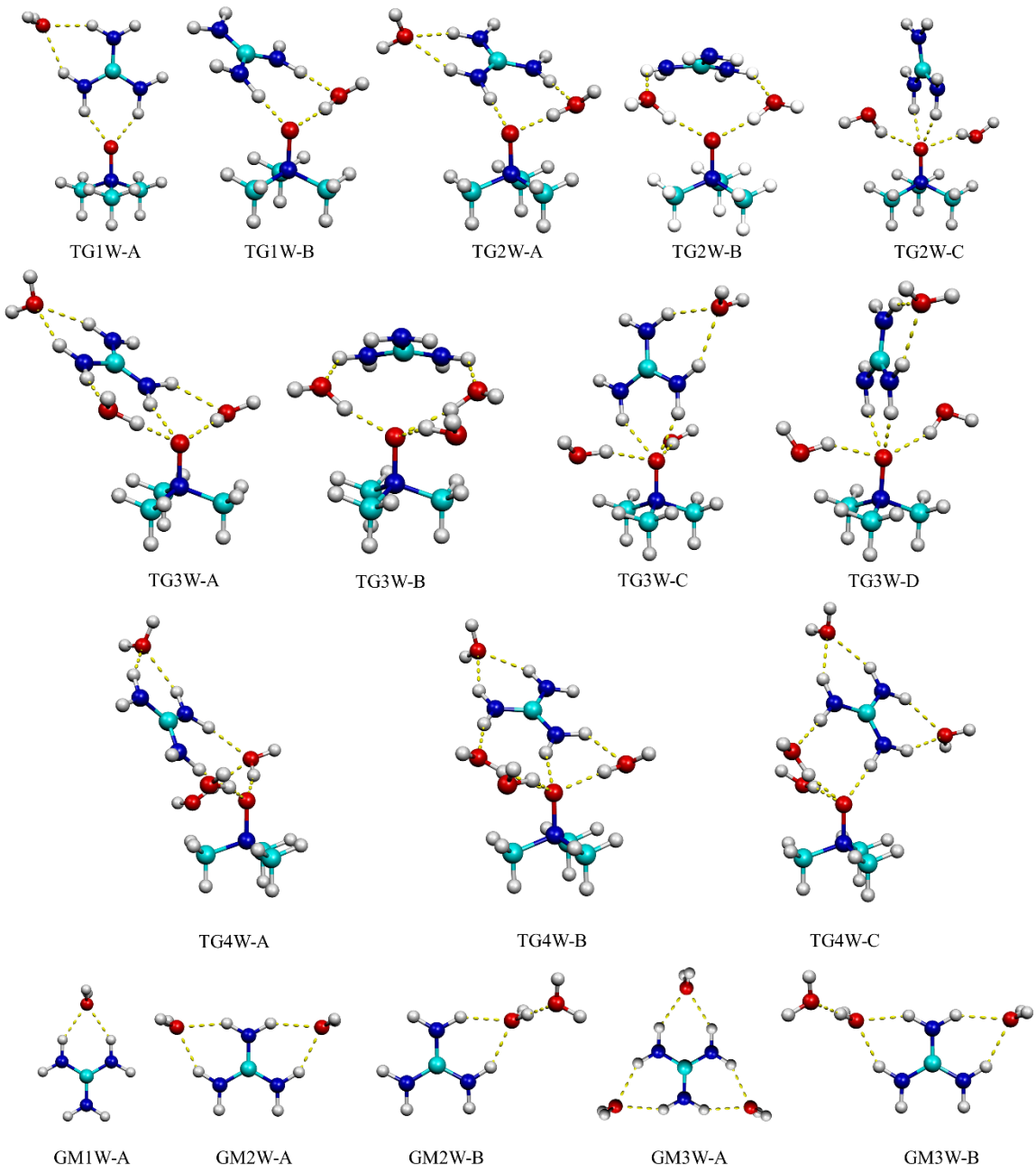

Figure 5.5 Optimized structures of TMAO and guanidinium with up to four water molecules.

Minimum Energy Structures	Relative Energies (kcal/mol)	
	aug-cc-pVDZ	aug-cc-pVTZ
TMAO-Guanidinium-1 Water		
TG1W-A	0.00	0.00
TG1W-B	1.22	1.86
TMAO-Guanidinium-2 Waters		
TG2W-A	0.00	0.00
TG2W-B	0.02	2.18
TG2W-C	--	10.08
TMAO-Guanidinium-3 Waters		
TG3W-A	0.00	0.00
TG3W-B	1.76	5.10
TG3W-C	5.14	7.74
TG3W-D	5.10	7.81
Guanidinium-1 Water		
G1W-A	0.00	0.00
Guanidinium-2 Waters		
G2W-A	0.00	0.00
G2W-B	3.42	3.12
Guanidinium-3 Waters		
G3W-A	0.00	0.00
G3W-B	2.32	2.61

Table 5.1. Relative energies in kcal/mol of the minimum energy TMAO/guanidinium/water structures using the M06-2X density functional and either aug-cc-pVDZ and aug-cc-pVTZ basis sets (ZPE correction was applied to the energies).

In most cases with the TMAO/guanidinium/water molecular clusters, there exists one or more water molecules hydrogen bonded to the oxygen atom of TMAO. This is consistent with our previous study where we examined noncovalent interactions in the hydrogen bond networks of TMAO.[55, 56] Good agreement between experiment and theory previously illustrated the importance of TMAO's oxygen atom in directing the structure of hydrogen-bonded networks, as TMAO's oxygen atom accepts three hydrogen bonds from water molecules on average.[55, 56] With the exception of the lowest energy conformation with one water molecule, the lowest energy conformations for TMAO/guanidinium/water clusters all have at least one water molecule hydrogen bonded to TMAO's oxygen atom. Moreover, the water molecule is also hydrogen bonded to a hydrogen atom from one of guanidinium's nitrogen atoms. On the other hand, the lowest energy conformation for guanidinium/water clusters have water's oxygen atom hydrogen bonded with two hydrogens from one of guanidinium's nitrogen atoms. This remains the case for up to three water molecules.

Figure 5.6 compares the simulated Raman spectra of the lowest energy conformation of TMAO, guanidinium, and three waters, to that of hydrated guanidinium with three waters in the H-N-H bending region of guanidinium.

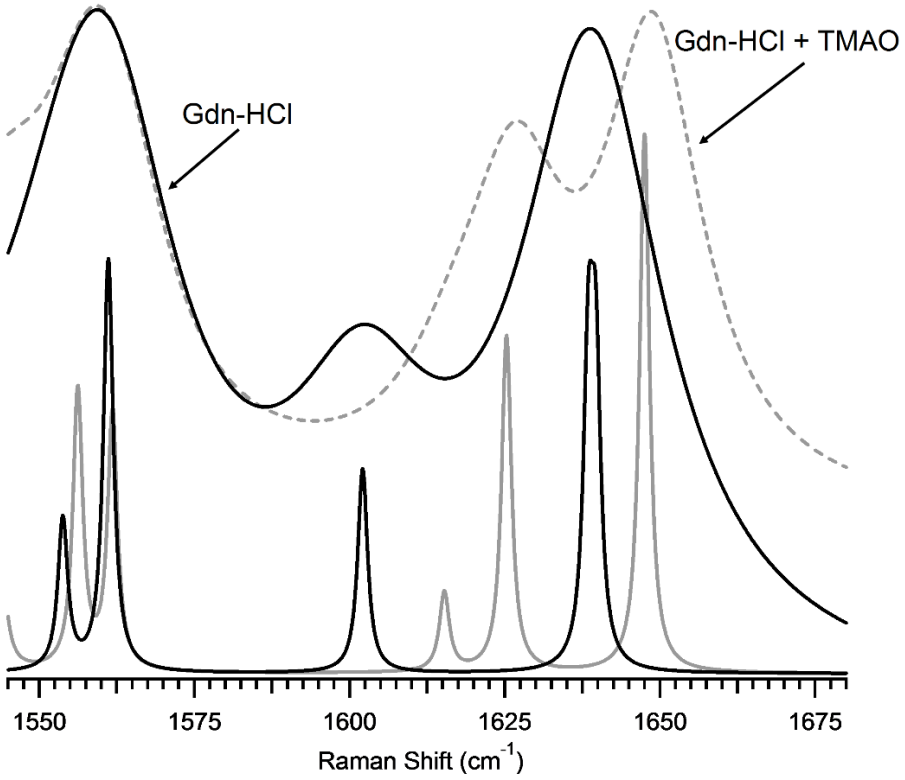

Figure 5.6 Simulated Raman spectra of TG3W-A (dotted gray) compared to GM3W-A (solid black).

The simulated Raman spectra were created by using optimized equilibrium geometries of molecular clusters from M06-2X/aug-cc-pVTZ harmonic vibrational frequencies and summing Lorentzian functions for each normal mode. The lowest energy configuration with the most waters - in this case TGM3-A - is most likely to exhibit properties that most closely match experimental data obtained at room

temperature.[147, 178] Frequencies were scaled using a correction factor of 0.984 in order to partially correct for anharmonicity.[180] Figure 5.6 includes simulated spectra using linewidths similar to those observed experimentally and also narrower linewidths so that the individual contributions from normal modes can be visualized. While little to no shift is observed in the first broad feature centered at approximately 1560 cm^{-1}, there are obvious blue shifts observed in the higher energy features. The overall 8.8 cm^{-1} shift in the second broad feature agrees closely with the 8.6 cm^{-1} shift observed experimentally.

5.7 Discussion

Hydration studies performed on the guanidinium cation by Cooper et al. demonstrated that water-water bonding becomes preferred over water-ion bonding when four or more water molecules are present.[166] In turn, a second hydration shell is created, suggesting that the cation is weakly hydrated.[166] Here, for TG3W-A, the lowest energy conformation for the osmolyte pair interacting with three water molecules, two water molecules form hydrogen bonds with TMAO's oxygen atom and two of guanidinium's NH_2 groups. Conversely, when another water molecule is added to guanidinium (GM3W-A), all of guanidinium's NH_2 groups have water molecules hydrogen bonded to them, filling all of guanidinium's available binding

sites. When a fourth water molecule is added to TMAO and guanidinium (TG4W-A), the additional water molecule preferentially forms a hydrogen bond with another water molecule over hydrogen bonding with one of guanidinium's binding sites.

In isolation, the guanidinium ion has a Raman-active asymmetric degenerate mode around 1600 cm^{-1},[181, 182] which can be seen in Figure 5.6. Vorobyev et al. examined this degenerate mode previously using ultrafast vibrational spectroscopy, and later ultrafast 2D IR Echo spectroscopy.[181, 182] This degenerate mode was found to correspond to a CN_3 stretch and NH_2 scissor motions.[182] A later study by Vorobyev et al. on the water-induced relaxation of guanidinium's degenerate mode suggested that NH_2 groups bend out of plane and wag rapidly due to interactions with surrounding water molecules. The corresponding frequencies of this degenerate mode can be correlated with the configuration of guanidinium's NH_2 groups.[182] While previous studies have sought to elucidate the hydration of guanidinium, the micro-solvation of TMAO, and the effects of TMAO on other osmolytes, namely urea, few studies have focused on TMAO and guanidinium interactions. Our results suggest that adding TMAO to aqueous solutions containing guanidinium induces a blue shift in guanidinium's H-N-H bending motions. This implies a direct

interaction of both the NH_2 groups of the guanidinium and water with TMAO at high concentrations, causing a disruption of guanidinium's surrounding hydration shell. Blue shifting occurs as guanidinium's NH_2 groups act as hydrogen bond donors and as TMAO's oxygen acts as a hydrogen bond acceptor. Moreover, the lowest energy conformations of TMAO, guanidinium, and water illustrate the disruption of guanidinium's hydrogen bond network, as both water and guanidinium directly interact with TMAO.

5.8 Conclusions

The effects of TMAO and guanidinium chloride on the hydrogen bond network of water were investigated using Raman Spectroscopy and DFT calculations. Good agreement between experimental and theoretical results suggests that TMAO and guanidinium interact directly in solution at high concentrations. When TMAO is added to guanidinium in aqueous solution, a blue shift occurs in guanidinium's H-N-H bending region. These findings support previous studies on urea and guanidinium, suggesting that both of these osmolytes destabilize proteins in a similar fashion, disrupting existing water-water networks in an indirect mechanism.

5.9 Note

This work was submitted to the *Journal of Raman Spectroscopy* in February 2020, and it is currently in revision. Professor David Magers, Mary Hannah Byrd, and Professor Shelley A. Smith (Mississippi College) performed full geometry optimizations and corresponding harmonic frequency calculations included in this thesis. I then used that data to create simulated spectra.

CHAPTER 6

REFERENCES

1. OpenStax, Chapter 2.0 Chemical Level of Organization. In *Anatomy and Physiology*, Rice University: 2013.

2. Tro, N., J., *Chemistry: Structure and Properties*. Pearson, 2015.

3. OpenStax, Chapter 7 Chemical Bonding and Molecular Geometry. In *Chemistry* 2nd ed.; OpenStax, 2019.

4. OpenStax, Chapter 8. Advanced Theories of Covalent Bonding. In *Chemistry*, 2nd ed.; OpenStax, 2018.

5. Vining, B., Chapter 9: Theories of Chemical Bonding Oneonta, S., Ed. 2019.

6. Müller-Dethlefs, K.; Hobza, P., Noncovalent Interactions: A Challenge for Experiment and Theory. *Chemical Reviews* **2000,** *100* (1), 143-168.

7. Casiday, R.; Frey, R., Hemoglobin and the Heme Group: Metal Complexes in the Blood for Oxygen Transport Washington University of St. Louis: 2007.

8. Feng, B.; Sosa, R. P.; Mårtensson, A. K. F.; Jiang, K.; Tong, A.; Dorfman, K. D.; Takahashi, M.; Lincoln, P.; Bustamante, C. J.; Westerlund, F.; Nordén, B., Hydrophobic catalysis and a potential biological role of DNA

unstacking induced by environment effects. *Proceedings of the National Academy of Sciences* **2019,** *116* (35), 17169-17174.

9. Ghosh, D.; Kosenkov, D.; Vanovschi, V.; Williams, C. F.; Herbert, J. M.; Gordon, M. S.; Schmidt, M. W.; Slipchenko, L. V.; Krylov, A. I., Noncovalent Interactions in Extended Systems Described by the Effective Fragment Potential Method: Theory and Application to Nucleobase Oligomers. *The Journal of Physical Chemistry A* **2010,** *114* (48), 12739-12754.

10. Tschumper, G. S., Reliable Electronic Structure Computations for Weak Noncovalent Interactions in Clusters. In *Reviews in Computational Chemistry*, pp 39-90.

11. OpenStax, Chapter 10 Liquids and Solids. In *Chemistry*, 2nd ed.; OpenStax, 2017.

12. Smith, D. A., A Brief History of the Hydrogen Bond. In *Modeling the Hydrogen Bond*, American Chemical Society: 1994; Vol. 569, pp 1-5.

13. Latimer, W. M.; Rodebush, W. H., Polarity and Ionization from the Standpoint of the Lewis Theory of Valence. *Journal of the American Chemical Society* **1920,** *42* (7), 1419-1433.

14. Arunan, E.; Desiraju, G.; Klein, R.; Sadlej, J.; Scheiner, S.; Alkorta, I.; Clary, D.; Crabtree, R.; Dannenberg, J.; Hobza, P.; Kjaergaard, H. G.; Legon, A.;

Mennucci, B.; Nesbitt, D., Definition of the Hydrogen Bond (IUPAC Recommendations 2011). *Pure & Appl.Chem.* **2011,** *83*, 1637-1641.

15. Lee, H. R.; Helquist, S. A.; Kool, E. T.; Johnson, K. A., Importance of hydrogen bonding for efficiency and specificity of the human mitochondrial DNA polymerase. *J Biol Chem* **2008,** *283* (21), 14402-14410.

16. USGS, Water Q&A: Why is water the "universal solvent"? U.S. Geological Survey: 2020; Vol. 2020.

17. Michael, A., Water as the Universal Solvent. Pennsylvania State University 2018; Vol. 2020.

18. Ophardt, C. E., Intermolecular Forces: Hydrogen Bonding In *Virtual Chembook*, Elmhurst College: 2003.

19. Chaplan, M., Hydrogen Bonding in Water. London South Bank University 2019.

20. Tokmakoff, A., Interaction of Light With Matter. University of Chicago: 2020.

21. Keith, N.; Twardowski, M., 5.35 Introduction to Experimental Chemistry. Massachusetts Institute of Technology: MIT OpenCourseWare, Fall 2012.

22. OpenStax, Chapter 6: Photons and Matter Waves. In *University Physics*, OpenStax, 2016; Vol. 3.

23. Granger, R. M.; Yochum, H. M.; Granger, J. N.; Sienerth, K. D., *Instrumental Analysis*. Oxford University Press: 2017.

24. Butcher, G., *Tour of the Electromagnetic Spectrum* Third ed.; National Aeronautics and Space Administration 2016.

25. Ramsden, E. N., *A-Level Chemistry*. Fourth ed.; Nelson Thornes Publisher 2000.

26. Abozenadah, H., Bishop, A., Bittner, S. and Flatt, P.M, Chapter 4: Covalent Bonds and Molecular Compounds. In *Preparatory Chemistry* Western Oregon University 2017.

27. Griffin, R.; Voorhis, T. V., 5.61 Physical Chemistry: The Harmonic Oscillator. Massachusetts Institute of Technology: MIT OpenCourseWare, Fall 2007.

28. Misra, A., GG 711, Advanced Techniques in Geophysics and Materials Science: Vibrational Spectroscopy. University of Hawaii: Hawaii Institutes of Geophysics and Planetology 2011.

29. Tokmakoff, A.; Gheorghiu, M., Advanced Chemical Experimentation and Instrumentation: Molecular Spectroscopy of Acetylene and Methane. In *Massachusetts Institute of Technology*, MIT OpenCourseWare, Fall 2007.

30. Chapter 6: Raman Spectroscopy California Institute of Technology: BI Laser Resource Center 2009.

31. Sevian, H., Elementary Physics II: Electromagnetic Waves. Boston University 2000.

32. Willock, D., *Molecular Symmetry*. Wiley: 2009.

33. Potma, E. O.; Mukamel, S., *Coherent Raman Scattering Microscopy*. CRC Press/ Taylor & Francis Group, LLC: 2013.

34. Neese, F.; Bredow, T.; Wennmohs, F., Introduction to Computational Chemistry: Fundamentals and Goals of Computational Chemistry. Universität Bonn: 2007.

35. Morin, D., *Introduction to Classical Mechanics*. Cambridge University Press: 2005.

36. Hod, O., Molecules: The Born-Oppenheimer Approximation. Tel-Aviv University: 2010.

37. Iyengar, S. S., The Born-Oppenheimer approximation, the Many Electron Hamiltonian and the molecular Schrodinger Equation. Indiana University C561, Atomic and Molecular Quantum Theory 2020.

38. Feiguin, A. E., The Born-Oppenheimer approximation. Northeastern University Northeastern University Department of Physics 2009.

39. Parkinson, W., *What's the Matter with Waves?: An Introduction to Techniques and Applications of Quantum Mechanics*. Morgan & Claypool Publishers: 2018.

40. Weckman, T., Chem-E4110, Quantum Mechanics and Spectroscopy: Hartree–Fock theory. Aalto University: Department of Chemistry.

41. Sherrill, D. C., An Introduction to Hartree-Fock Molecular Orbital Theory. Georgia Institute of Technology: School of Chemistry and Biochemistry, 2000.

42. McQuarrie, D. A., *Quantum Chemistry*. University Science Books: 2008.

43. Burk, K., The ABC of DFT. University of California Irvine: Department of Chemistry, 2007.

44. Kahn, K., Semiempirical Quantum Chemistry. University of California Santa Barbara: Department of Chemistry and Biochemistry 2007.

45. Shell, S. M., Ab initio and electronic structure methods. University of California Santa Barbara: 2012.

46. Sherrill, D. C., Basis Sets in Quantum Chemistry. Georgia Institute of Technology: Chem 6485: Computational Chemistry, 2008.

47. Sherrill, D. C., Chem 6485, Background: Basis Sets. Georgia Institute of Technology: Sherrill Research Group Website 2009.

48. Sholl, D.; Steckel, J., *Density Functional Theory: A Practical Introduction* John Wiley & Sons: 2009.

49. Drake, G. W. F., *Springer Handbook of Atomic, Molecular, and Optical Physics*. Illustrated ed.; 2006.

50. Tsirelson, V. G.; Ozerov, R. P., *Electron Density and Bonding in Crystals: Principles, Theory and X-ray Diffraction Experiments in Solid State Physics and Chemistry*. Illustrated ed.; CRC Press: 1996.

51. Zhao, Y.; Truhlar, D. G., Density Functional for Spectroscopy: No Long-Range Self-Interaction Error, Good Performance for Rydberg and Charge-Transfer States, and Better Performance on Average than B3LYP for Ground States. *Journal of Physical Chemistry A* **2006,** *110* (49), 13126–13130.

52. Hohenberg, P.; Kohn, W., Inhomogeneous Electron Gas. *Physical Review* **1964,** *136* (3B), B864-B871.

53. Kohn, W.; Sham, L. J., Self-Consistent Equations Including Exchange and Correlation Effects. *Physical Review* **1965,** *140* (4A), A1133-A1138.

54. Jr., T. H. D., Gaussian basis sets for use in correlated molecular calculations. I. The atoms boron through neon and hydrogen. *The Journal of Chemical Physics* **1989,** *90* (2), 1007-1023.

55. Cuellar, K. A.; Munroe, K. L.; Magers, D. H.; Hammer, N. I., Noncovalent Interactions in Microsolvated Networks of Trimethylamine N-Oxide. *Journal of Physical Chemistry B* **2014,** *118* (2), 449–459.

56. Munroe, K. L.; Magers, D. H.; Hammer, N. I., Raman Spectroscopic Signatures of Noncovalent Interactions Between Trimethylamine N-oxide (TMAO) and Water. *Journal of Physical Chemistry B* **2011,** *115* (23), 7699-7707.

57. Howard, J. C.; Hammer, N. I.; Tschumper, G. S., Structures, energetics and vibrational frequency shifts of hydrated pyrimidine. *ChemPhysChem* **2011,** *12* (17), 3262-73.

58. Howard, A. A.; Tschumper, G. S.; Hammer, N. I., Effects of Hydrogen Bonding on Vibrational Normal Modes of Pyrimidine. *Journal of Physical Chemistry A* **2010,** *114* (25), 6803-6810.

59. Wright, A. M.; Howard, A. A.; Howard, J. C.; Tschumper, G. S.; Hammer, N. I., Charge Transfer and Blue Shifting of Vibrational Frequencies in a Hydrogen Bond Acceptor. *Journal of Physical Chemistry A* **2013,** *117* (26), 5435-5446.

60. Kocherbitov, V. V., V.; Soderman, O. J., Hydration of Trimethylamine-N-Oxide and of Dimethyldodecylamine-N-Oxide: An ab initio Study. *Mol. Struc. Theochem* **2007,** *808*, 111-118.

61. Walker, M.; Harvey, A. J. A.; Sen, A.; Dessent, C. E. H., Performance of M06, M06-2X, and M06-HF Density Functionals for Conformationally Flexible Anionic Clusters: M06 Functionals Perform Better than B3LYP for a Model System with Dispersion and Ionic Hydrogen-Bonding Interactions. *The Journal of Physical Chemistry* **A 2013,** *117* (47), 12590-12600.

62. Zhang, Y.; Ma, N.; Wang, W., Assessment of the Performance of the M05-Class and M06-Class Functionals for the Structure and Geometry of the Hydrogen-Bonded and Halogen-Bonded Complexes. *Journal of Theoretical and Computational Chemistry* **2012,** *11* (06), 1165-1173.

63. Schneebeli, S. T.; Bochevarov, A. D.; Friesner, R. A., Parameterization of a B3LYP specific correction for non-covalent interactions and basis set superposition error on a gigantic dataset of CCSD(T) quality non-covalent interaction energies. *Journal of Chemical Theory and Computation* **2011,** *7* (3), 658-668.

64. Liu, Y.; Zhao, J.; Li, F.; Chen, Z., Appropriate description of intermolecular interactions in the methane hydrates: An assessment of DFT methods. *Journal of Computational Chemistry* **2013,** *34* (2), 121-131.

65. Scardino, D. J.; Howard, A. A.; McDowell, M. D.; Hammer, N. I., Raman Spectroscopy as the Method of Detection for Constructing a Binary Liquid-Vapor Phase Diagram. *Journal of Chemical Education* **2011,** *88* (8), 1162-1165.

66. Garcia-Perez, A.; Burg, M. B., Importance of organic osmolytes for osmoregulation by renal medullary cells. *Hypertension* **1990,** *16* (6), 595-602.

67. Yancey, P. H.; Somero, G. N., Counteraction of urea destabilization of protein structure by methylamine osmoregulatory compounds of elasmobranch fishes. *Biochem J* **1979,** *183* (2), 317-23.

68. Yancey, P. H.; Clark, M. E.; Hand, S. C.; Bowlus, R. D.; Somero, G. N., Living with Water Stress: Evolution of Osmolyte Systems. *Science* **1982,** *217* (4566), 1214-1222.

69. Roseman, M.; Jencks, W. P., Interactions of Urea and Other Polar Compounds in Water. *Journal of the American Chemical Society* **1975,** *97* (3), 631-640.

70. Tanford, C., The Hydrophobic Effect. Wiley: New York, 1980.

71. Wallqvist, A.; Covell, D. G.; Thirumalai, D., Hydrophobic Interactions in Aqueous Urea Solutions with Implications for the Mechanism of Protein Denaturation. *Journal of the American Chemical Society* **1998,** *120* (2), 427-428.

72. Ikeguchi, M.; Nakamura, S.; Shimizu, K., Molecular Dynamics Study on Hydrophobic Effects in Aqueous Urea Solutions. *Journal of the American Chemical Society* **2001,** *123* (4), 677-682.

73. Sharp, K. A.; Madan, B.; Manas, E.; Vanderkooi, J. M., Water Structure Changes Induced by Hydrophobic and Polar Solutes Revealed by Simulations and Infrared Spectroscopy. *Journal of Chemical Physics* **2001,** *114*, 1791.

74. Weerasinghe, S.; Smith, P. E., A Kirkwood-Buff Derived Force Field for Mixtures of Urea and Water. *Journal of Physical Chemistry B* **2003,** *107* (16), 3891-3898.

75. Batchelor, J. D.; Olteanu, A.; Tripathy, A.; Pielak, G. J., Impact of Protein Denaturants and Stabilizers on Water Structure. *Journal of the American Chemical Society* **2004,** *126* (7), 1958-1961.

76. Street, T. O.; Bolen, D. W.; Rose, G. D., A Molecular Mechanism for Osmolyte-Induced Protein Stability. *Proceedings of the National Academy of Sciences of the United States of America* **2006,** *103* (38), 13997-14002.

77. Paul, S.; Patey, G. N., Structure and Interaction in Aqueous Urea - Trimethylamine-N-oxide solutions. *Journal of the American Chemical Society* **2007,** *129* (14), 4476-4482.

78. Paul, S.; Patey, G. N., The Influence of Urea and Trimethylamine-N-oxide on Hydrophobic Interactions. *Journal of Physical Chemistry B* **2007,** *111* (28), 7932-7933.

79. Paul, S.; Patey, G. N., Hydrophobic Interactions in Urea-Trimethylamine-N-oxide solutions. *Journal of Physical Chemistry B* **2008,** *112* (35), 11106-11111.

80. Meersman, F.; Bowron, D.; Soper, A. K.; Koch, M. H. J., Counteraction of Urea by Trimethylamine N-oxide is Due to Direct Interaction. *Biophysical Journal* **2009,** *97* (9), 2559-2566.

81. Panuszko, A.; Bruzdziak, P.; Zielkiewicz, J.; Wyrzykowski, D.; Stangret, J., Complex Formation in Aqueous Trimethylamine-N-oxide (TMAO) Solutions. *Journal of Physical Chemistry B* **2009,** *113*, 4783–4795.

82. Zangi, R.; Zhou, R.; Berne, B. J., Urea's Action on Hydrophobic Interactions. *Journal of the American Chemical Society* **2009,** *131* (4), 1535-1541.

83. Kuffel, A.; Zielkiewicz, J., The hydrogen bond network structure within the hydration shell around simple osmolytes: Urea, tetramethylurea, and trimethylamine-N-oxide, investigated using both a fixed charge and a polarizable water model. *The Journal of Chemical Physics* **2010,** *133* (3), 035102.

84. Wei, H.; Fan, Y.; Gao, Y. Q., Effects of Urea, Tetramethyl Urea, and Trimethylamine N-Oxide on Aqueous Solution Structure and Solvation of Protein Backbones: A Molecular Dynamics Simulation Study. *Journal of Physical Chemistry B* **2010** *114* (1), 557-568.

85. Meersman, F.; Bowron, D.; Soper, A. K.; Koch, M. H. J., An X-ray and neutron scattering study of the equilibrium between trimethylamine N-oxide and urea in aqueous solution. *Physical Chemistry Chemical Physics* **2011,** *13* (30), 13765-13771.

86. Sarma, R.; Paul, S., Hydrophobic Interactions in Presence of Osmolytes Urea and Trimethylamine-N-Oxide. *Journal of Chemical Physics* **2011,** *135* (17), 174501.

87. Rösgen, J.; Jackson-Atogi, R., Volume Exclusion and H-Bonding Dominate the Thermodynamics and Solvation of Trimethylamine-N-Oxide in Aqueous Urea. *Journal of the American Chemical Society* **2012,** *134* (7), 3590-3597.

88. Mondal, J.; Stirnemann, G.; Berne, B. J., When Does Trimethylamine N-Oxide Fold a Polymer Chain and Urea Unfold It? *Journal of Physical Chemistry B* **2013,** *117* (29), 8723-8732.

89. Sarma, R.; Paul, S., Exploring the molecular mechanism of trimethylamine-N-oxide's ability to counteract the protein denaturing effects of urea. *Journal of Physical Chemistry B* **2013,** *117* (18), 5691-5704.

90. Ma, J.; Pazos, I. M.; Gai, F., Microscopic Insights Into the Protein-Stabilizing Effect of Trimethylamine N-Oxide (TMAO). *Proceedings of the National Academy of Sciences of the United States of America* **2014** *111* (23), 8476-8481.

91. Hunger, J.; Ottosson, N.; Mazur, K.; Bonn, M.; Bakker, H. J., Water-Mediated Interactions Between Trimethylamine-N-Oxide and Urea. *Physical Chemistry Chemical Physics* **2013,** *17* (1), 298-306.

92. Borgohain, G.; Paul, S., Model Dependency of TMAO's Counteracting Effect Against Action of Urea: Kast Model versus Osmotic Model of TMAO. *Journal of Physical Chemistry B* **2016,** *120* (9), 2352–2361.

93. Ganguly, P.; van der Vegt, N. F. A.; Shea, J.-E., Hydrophobic Association in Mixed Urea–TMAO Solutions. *The Journal of Physical Chemistry Letters* **2016,** *7* (15), 3052-3059.

94. Ohto, T.; Hunger, J.; Backus, E. H. G.; Mizukami, W.; Bonn, M.; Nagata, Y., Trimethylamine-N-Oxide: Its Hydration Structure, Surface Activity, and Biological Function, Viewed by Vibrational Spectroscopy and Molecular Dynamics Simulations. *Physical Chemistry Chemical Physics* **2017,** *19* (10), 6909-6920.

95. Smolin, N.; Voloshin, V. P.; Anikeenko, A. V.; Geiger, A.; Winter, R.; Medvedev, N. N., TMAO and Urea in the Hydration Shell of the Protein SNase. *Physical Chemistry Chemical Physics* **2017,** *19* (9), 6345-6357.

96. Van Der Vegt, N. F. A.; Nayar, D., The Hydrophobic Effect and the Role of Cosolvents. *Journal of Physical Chemistry B* **2017,** *121* (43), 9986-9998.

97. Yancey, P. H., Organic Osmolytes as Compatible, Metabolic and Counteracting Cytoprotectants in High Osmolarity and Other Stresses. *Journal of Experimental Biology* **2005,** *208* (15), 2819-2830.

98. Watlaufer, D. B.; Malik, S. K.; Stoller, L.; Coffin, R. L., Nonpolar Group Participation in the Denaturation of Proteins by Urea and Guanidinium Salts. Model Compound Studies. *Journal of the American Chemical Society* **1964,** *86* (3), 508-514.

99. Bennion, B. J.; Daggett, V., The Molecular Basis for the Chemical Denaturation of Proteins by Urea. *Proceedings of the National Academy of Sciences of the United States of America* **2003,** *100* (9), 5142-5147.

100. Lee, M. E.; Van Der Vegt, N. F. A., Does Urea Denature Hydrophobic Interactions? *Journal of the American Chemical Society* **2006,** *128* (15), 4948-4949.

101. Auton, M.; Holthauzen, L. M. F.; Bolen, D. W., Anatomy of Energetic Changes Accompanying Urea-Induced Protein Denaturation. *Proceedings of the National Academy of Sciences of the United States of America* **2007,** *104* (39), 15317-15322.

102. Hua, L.; Zhou, R.; Thirumalai, D.; Berne, B. J., Urea denaturation by stronger dispersion interactions with proteins than water implies a 2-stage unfolding. *Proceedings of the National Academy of Sciences* **2008,** *105* (44), 16928-16933.

103. Canchi, D. R.; Paschek, D.; Garcia, A. E., Equilibrium Study of Protein Denaturation by Urea. *Journal of the American Chemical Society* **2010,** *132* (7), 2338-2344.

104. Guinn, E. J.; Pegram, L. M.; Capp, M. W.; Pollock, M. N.; Record Jr, M. T., Quantifying Why Urea is a Protein Denaturant, Whereas Glycine Betaine is a

Protein Stabilizer. *Proceedings of the National Academy of Sciences of the United States of America* **2011,** *108* (41), 16932-16937.

105. Rossky, P. J., Protein Denaturation by Urea: Slash and Bond. *Proceedings of the National Academy of Sciences of the United States of America* **2008,** *105* (44), 16825-16826.

106. Moeser, B.; Horinek, D., Unified Description of Urea Denaturation: Backbone and Side Chains Contribute Equally in the Transfer Model. *Journal of Physical Chemistry B* **2014** *118* (1), 107-114.

107. Wei, H.; Fan, Y.; Gao, Y. Q., Effects of Urea, Tetramethyl Urea, and Trimethylamine N-Oxide on Aqueous Solution Structure and Solvation of Protein Backbones: A Molecular Dynamics Simulation Study. *The Journal of Physical Chemistry B* **2010,** *114* (1), 557-568.

108. Bolen, D. W.; Rose, G. D., Structure and Energetics of the Hydrogen-Bonded Backbone in Protein Folding. In *Annual Review of Biochemistry*, 2008; Vol. 77, pp 339-362.

109. Zhang, Y. J. C., P. S, Chemistry of Hofmeister Anions and Osmolytes. *Annual Rev. Phys. Chem* **2010,** *61*, 63-83.

110. Canchi, D. R.; García, A. E., Cosolvent Effects on Protein Stability. In *Annual Review of Physical Chemistry*, 2013; Vol. 64, pp 273-293.

111. Athawale, M. V.; Dordick, J. S.; Garde, S., Osmolyte Trimethylamine-N-Oxide Does Not Affect the Strength of Hydrophobic Interactions: Origin of Osmolyte Compatibility. *Biophysical Journal* **2005,** *89* (2), 858-866.

112. Ma, J.; Pazos, I. M.; Gai, F., Microscopic insights into the protein-stabilizing effect of trimethylamine N-oxide (TMAO). *Proc Natl Acad Sci U S A* **2014,** *111* (23), 8476-81.

113. Canchi, D. R.; Jayasimha, P.; Rau, D. C.; Makhatadze, G. I.; Garcia, A. E., Molecular Mechanism for the Preferential Exclusion of TMAO from Protein Surfaces. *Journal of Physical Chemistry B* **2012,** *116* (40), 12095-12104.

114. Sagle, L. B. C., K.; Litosh, V. A.; Liu, Y.; Flores, S. C.; Chen, X.; Yu, B.; Cremer, P. S., Methyl Groups of Trimethylamine N-Oxide Orient Away from Hydrophobic Interfaces. *Journal of the American Chemical Society* **2011,** *133*, 18707-18712.

115. Wang, A.; Bolen, D. W., A Naturally Occurring Protective System in Urea-Rich Cells: Mechanism of Osmolyte Protection of Proteins Against Urea Denaturation. *Biochemistry* **1997,** *36* (30), 9101-9108.

116. Qu, Y.; Bolen, D. W., Hydrogen exchange kinetics of RNase A and the urea:TMAO paradigm. *Biochemistry* **2003,** *42* (19), 5837-49.

117. Yancey, P. H.; Somero, G. N., Counteraction of Urea Destabilization of Protein Structure by Methylamine Osmoregulatory Compounds of Elasmobranch Fishes. *Biochemical Journal* **1979,** *183* (2), 317-323.

118. Ganguly, P.; Boserman, P.; Van Der Vegt, N. F. A.; Shea, J. E., Trimethylamine N-oxide Counteracts Urea Denaturation by Inhibiting Protein-Urea Preferential Interaction. *Journal of the American Chemical Society* **2018,** *140* (1), 483-492.

119. Sahle, C. J.; Schroer, M. A.; Juurinen, I.; Niskanen, J., Influence of TMAO and Urea on the Structure of Water Studied by Inelastic X-ray Scattering. *Physical Chemistry Chemical Physics* **2016,** *18* (24), 16518-16526.

120. Karpfen, A., Blue-Shifted A–H Stretching Frequencies in Complexes with Methanol: the Decisive Role of Intramolecular Coupling. *Physical Chemistry Chemical Physics* **2011,** *13*, 14194-14201.

121. Kelly, J. T.; McClellan, A. K.; Joe, L. V.; Wright, A. M.; Lloyd, L. T.; Tschumper, G. S.; Hammer, N. I., Competition between Hydrophilic and Argyrophilic Interactions in Surface Enhanced Raman Spectroscopy. *ChemPhysChem* **2016,** *17* (18), 2782-2786.

122. Ellington, T. L.; Reves, P. L.; Simms, B. L.; Wilson, J. L.; Watkins, D. L.; Tschumper, G. S.; Hammer, N. I., Quantifying the Effects of Halogen Bonding by

Haloaromatic Donors on the Acceptor Pyrimidine. *ChemPhysChem* **2017,** *18* (10), 1267-1273.

123. Parr, R. G. Y., W., Density Functional Theory of Atoms and Molecules. *Oxford University Press* **1989**.

124. Kendall, R. A.; Dunning Jr., T. H.; Harrison, R. J., Electron Affinities of the First-Row Atoms Revisited. Systematic Basis Sets and Wave Functions. *Journal of Chemical Physics* **1992,** *96*, 6796.

125. Frisch, M. J. T., G. W.; Schlegel, H. B.; et. al *Gaussian 09*, Gaussian, Inc: Wallingford, CT, USA, 2009.

126. Hayashi, Y.; Katsumoto, Y.; Omori, S.; Kishii, N.; Yasuda, A., Liquid Structure of the Urea - Water System Studied by Dielectric Spectroscopy. *Journal of Physical Chemistry B* **2007,** *111* (5), 1076-1080.

127. Rezus, Y. L. A.; Bakker, H. J., Effect of Urea on the Structural Dynamics of Water. *Proceedings of the National Academy of Sciences of the United States of America* **2006,** *103* (49), 18417-18420.

128. Hermida-Ramón, J. M.; Öhrn, A.; Karlström, G., Planar or Nonplanar: What is the Structure of Urea in Aqueous Solution? *Journal of Physical Chemistry B* **2007,** *111* (39), 11511-11515.

129. Idrissi, A.; Gerard, M.; Damay, P.; Kiselev, M.; Puhovsky, Y.; Cinar, E.; Lagant, P.; Vergoten, G., The Effect of Urea on the Structure of Water: A Molecular Dynamics Simulation. *Journal of Physical Chemistry B* **2010,** *114* (13), 4731-4738.

130. Carr, J. K.; Buchanan, L. E.; Schmidt, J. R.; Zanni, M. T.; Skinner, J. L., Structure and Dynamics of Urea/Water Mixtures Investigated by Vibrational Spectroscopy and Molecular Dynamics Simulation. *Journal of Physical Chemistry B* **2013,** *117* (42), 13291-13300.

131. Bandyopadhyay, D.; Mohan, S.; Ghosh, S. K.; Choudhury, N., Molecular Dynamics Simulation of Aqueous Urea Solution: Is Urea a Structure Breaker? *Journal of Physical Chemistry B* **2014,** *118* (40), 11757-11768.

132. Burakowski, A.; Gliński, J., Hydration of Urea and its Derivatives from Acoustic and Volumetric Methods. *Chemical Physics Letters* **2015,** *641*, 40-43.

133. Kokubo, H.; Hu, C. Y.; Pettitt, B. M., Peptide Conformational Preferences in Osmolyte Solutions: Transfer Free Energies of Decaalanine. *Journal of the American Chemical Society* **2011,** *133* (6), 1849-1858.

134. Zetterholm, S. G.; Verville, G. A.; Boutwell, L.; Boland, C.; Prather, J. C.; Bethea, J.; Cauley, J.; Warren, K. E.; Smith, S. A.; Magers, D. H.; Hammer, N.

I., Noncovalent Interactions between Trimethylamine N-Oxide (TMAO), Urea, and Water. *The Journal of Physical Chemistry B* **2018,** *122* (38), 8805-8811.

135. Garcia-Perez, A., Importance of Organic Osmolytes for Osmoregulation by Renal Medullary Cells. *Hypertension: Journal of the American Heart Association* **1990** *16* (7), 595-602.

136. Slama, I.; Abdelly, C.; Bouchereau, A.; Flowers, T.; Savouré, A., Diversity, distribution and roles of osmoprotective compounds accumulated in halophytes under abiotic stress. *Annual Bot.* **2015,** *115* (3), 433-47.

137. Krasensky, J.; Jonak, C., Drought, salt, and temperature stress-induced metabolic rearrangements and regulatory networks. *Journal of experimental botany* **2012,** *63* (4), 1593-1608.

138. Singh, R.; Haque, I.; Ahmad, F., Counteracting osmolyte trimethylamine N-oxide destabilizes proteins at pH below its pKa. Measurements of thermodynamic parameters of proteins in the presence and absence of trimethylamine N-oxide. *J Biol Chem* **2005,** *280* (12), 11035-42.

139. Goldstein, L.; Forster, R., Osmoregulation and urea metabolism in the little skate Raja erinacea. *American Journal of Physiology-Legacy Content* **1971,** *220* (3), 742-746.

140. Welch, W. J.; Brown, C. R., Influence of molecular and chemical chaperones on protein folding. *Cell Stress Chaperones* **1996,** *1* (2), 109-15.

141. Harries, D.; Rosgen, J., A practical guide on how osmolytes modulate macromolecular properties. *Methods Cell Biol* **2008,** *84*, 679-735.

142. Yancey, P. H., Water Stress, Osmolytes and Proteins1. *American Zoologist* **2001,** *41* (4), 699-709.

143. Macchi, F.; Eisenkolb, M.; Kiefer, H.; Otzen, D., *The Effect of Osmolytes on Protein Fibrillation*. 2012; Vol. 13, p 3801-19.

144. Zou, Q.; Bennion, B. J.; Daggett, V.; Murphy, K. P., The Molecular Mechanism of Stabilization of Proteins by TMAO and Its Ability to Counteract the Effects of Urea. *Journal of the American Chemical Society* **2002,** *124* (7), 1192-1202.

145. Lin, T.-Y.; Timasheff, S. N., Why do some organisms use a urea-methylamine mixture as osmolyte? Thermodynamic compensation of urea and trimethylamine N-oxide interactions with protein. *Biochemistry* **1994,** *33* (42), 12695-12701.

146. Ertell; Gb, K., *A Review of Toxicity and Use and Handling Considerations for Guanidine, Guanidine Hydrochloride, and Urea*. 2018.

147. Kumar, R.; Prabhu, N. P.; Yadaiah, M.; Bhuyan, A. K., Protein stiffening and entropic stabilization in the subdenaturing limit of guanidine hydrochloride. *Biophys J* **2004,** *87* (4), 2656-62.

148. O'Brien, E. P.; Dima, R. I.; Brooks, B.; Thirumalai, D., Interactions between hydrophobic and ionic solutes in aqueous guanidinium chloride and urea solutions: lessons for protein denaturation mechanism. *J Am Chem Soc* **2007,** *129* (23), 7346-53.

149. Chiba, T.; Hagihara, Y.; Higurashi, T.; Hasegawa, K.; Naiki, H.; Goto, Y., Amyloid fibril formation in the context of full-length protein: effects of proline mutations on the amyloid fibril formation of beta2-microglobulin. *J Biol Chem* **2003,** *278* (47), 47016-24.

150. Rani, A.; Venkatesu, P., A Distinct Proof on Interplay between Trehalose and Guanidinium Chloride for the Stability of Stem Bromelain. *The Journal of Physical Chemistry B* **2016,** *120* (34), 8863-8872.

151. Lim, W. K.; Rösgen, J.; Englander, S. W., Urea, but not guanidinium, destabilizes proteins by forming hydrogen bonds to the peptide group. *Proceedings of the National Academy of Sciences of the United States of America* **2009,** *106* (8), 2595-2600.

152. Hu, C. Y.; Pettitt, B. M.; Roesgen, J., Osmolyte solutions and protein folding. *F1000 Biology Reports* **2009,** *1*, 41.

153. Ferreira, L.; Breydo, L.; Reichardt, C.; Uversky, V.; Zaslavsky, B., *Effects of osmolytes on solvent features of water in aqueous solutions*. 2016; Vol. 35, p 1-41.

154. Attri, P.; Venkatesu, P.; Lee, M. J., Influence of osmolytes and denaturants on the structure and enzyme activity of alpha-chymotrypsin. *J Phys Chem B* **2010,** *114* (3), 1471-8.

155. Hunger, J.; Tielrooij, K.-J.; Buchner, R.; Bonn, M.; Bakker, H. J., Complex Formation in Aqueous Trimethylamine-N-oxide (TMAO) Solutions. *The Journal of Physical Chemistry B* **2012,** *116* (16), 4783-4795.

156. Rezus, Y. L. A.; Bakker, H. J., Destabilization of the Hydrogen-Bond Structure of Water by the Osmolyte Trimethylamine N-Oxide. *The Journal of Physical Chemistry B* **2009,** *113* (13), 4038-4044.

157. Rezus, Y. L.; Bakker, H. J., Observation of immobilized water molecules around hydrophobic groups. *Phys Rev Lett* **2007,** *99* (14), 1.

158. Burg, M. B.; Ferraris, J. D., Intracellular Organic Osmolytes: Function and Regulation. *J Biol Chem* **2008,** *283* (12), 7309-7313.

159. Bennion, B. J.; Daggett, V., Counteraction of urea-induced protein denaturation by trimethylamine N-oxide: A chemical chaperone at atomic resolution. *Proceedings of the National Academy of Sciences of the United States of America* **2004,** *101* (17), 6433-6438.

160. Yang, Y.; Mu, Y.; Li, W., Microscopic significance of hydrophobic residues in the protein-stabilizing effect of trimethylamine N-oxide (TMAO). *Physical Chemistry Chemical Physics* **2016** *18* (32), 22081-22088.

161. Mukherjee, M.; Mondal, J., Heterogeneous Impacts of Protein-Stabilizing Osmolytes on Hydrophobic Interaction. *The Journal of Physical Chemistry B* **2018,** *122* (27), 6922-6930.

162. Urbic, T., Ions increase strength of hydrogen bond in water. *Chemical Physics Letters* **2014,** *610-611*, 159-162.

163. Tanford, C., Protein denaturation. C. Theoretical models for the mechanism of denaturation. *Adv Protein Chem* **1970,** *24*, 1-95.

164. Frank, H. S.; Evans, M. W., Free Volume and Entropy in Condensed Systems III. Entropy in Binary Liquid Mixtures; Partial Molal Entropy in Dilute Solutions; Structure and Thermodynamics in Aqueous Electrolytes. *The Journal of Chemical Physics* **1945,** *13* (11), 507-532.

165. Mason, P. E.; Brady, J. W.; Neilson, G. W.; Dempsey, C. E., The Interaction of Guanidinium Ions with a Model Peptide. *Biophysical Journal* **2007,** *93* (1), L04-L06.

166. Cooper, R. J.; Heiles, S.; DiTucci, M. J.; Williams, E. R., Hydration of Guanidinium: Second Shell Formation at Small Cluster Size. *The Journal of Physical Chemistry A* **2014,** *118* (30), 5657-5666.

167. Camilloni, C.; Rocco, A. G.; Eberini, I.; Gianazza, E.; Broglia, R. A.; Tiana, G., Urea and Guanidinium Chloride Denature Protein L in Different Ways in Molecular Dynamics Simulations. *Biophysical Journal* **2008,** *94* (12), 4654-4661.

168. Heyda, J.; Okur, H. I.; Hladílková, J.; Rembert, K. B.; Hunn, W.; Yang, T.; Dzubiella, J.; Jungwirth, P.; Cremer, P. S., Guanidinium can both Cause and Prevent the Hydrophobic Collapse of Biomacromolecules. *Journal of the American Chemical Society* **2017,** *139* (2), 863-870.

169. Pazos, I. M.; Gai, F., Solute's Perspective on How Trimethylamine Oxide, Urea, and Guanidine Hydrochloride Affect Water's Hydrogen Bonding Ability. *The Journal of Physical Chemistry B* **2012** *116* (41), 12473-12478.

170. Samanta, N.; Mahanta, D. D.; Mitra, R. K., Collective hydration dynamics of guanidinium chloride solutions and its possible role in protein

denaturation: a terahertz spectroscopic study. *Physical Chemistry Chemical Physics* **2014,** *16* (42), 23308-23315.

171. Scott, J. N.; Nucci, N. V.; Vanderkooi, J. M., Changes in Water Structure Induced by the Guanidinium Cation and Implications for Protein Denaturation. *The journal of physical chemistry. A* **2008,** *112* (43), 10939-10948.

172. Schiffer, C. A.; Dotsch, V., The role of protein-solvent interactions in protein unfolding. *Curr Opin Biotechnol* **1996,** *7* (4), 428-32.

173. Vanzi, F.; Madan, B.; Sharp, K., Effect of the Protein Denaturants Urea and Guanidinium on Water Structure: A Structural and Thermodynamic Study. *Journal of the American Chemical Society* **1998,** *120* (41), 10748-10753.

174. Singh, L. R.; Dar, T. A., *Cellular Osmolytes: From Chaperoning Protein Folding to Clinical Perspectives*. Springer Singapore: 2017.

175. Liao, Y. T.; Manson, A. C.; DeLyser, M. R.; Noid, W. G.; Cremer, P. S., Trimethylamine N-oxide stabilizes proteins via a distinct mechanism compared with betaine and glycine. *Proc Natl Acad Sci U S A* **2017,** *114* (10), 2479-2484.

176. Bruzdziak, P.; Panuszko, A.; Stangret, J., Influence of osmolytes on protein and water structure: a step to understanding the mechanism of protein stabilization. *J Phys Chem B* **2013,** *117* (39), 11502-8.

177. Chai, J.-D.; Head-Gordon, M., Long-range corrected hybrid density functionals with damped atom–atom dispersion corrections. *Physical Chemistry Chemical Physics* **2008,** *10* (44), 6615-6620.

178. Cuypers, R.; Murali, S.; Marcelis, A. T. M.; Sudhölter, E. J. R.; Zuilhof, H., Complexation of Phenol and Thiophenol by Amine N-Oxides: Isothermal Titration Calorimetry and ab Initio Calculations. *ChemPhysChem* **2010,** *11* (16), 3465-3473.

179. Karpfen, A.; Kryachko, E. S., On blue shifts of C–H stretching modes of dimethyl ether in hydrogen- and halogen-bonded complexes. *Chemical Physics Letters* **2006,** *431* (4), 428-433.

180. Alecu, I. M.; Zheng, J.; Zhao, Y.; Truhlar, D. G., Computational Thermochemistry: Scale Factor Databases and Scale Factors for Vibrational Frequencies Obtained from Electronic Model Chemistries. *Journal of Chemical Theory and Computation* **2010,** *6* (9), 2872-2887.

181. Vorobyev, D. Y.; Kuo, C.-H.; Chen, J.-X.; Kuroda, D. G.; Scott, J. N.; Vanderkooi, J. M.; Hochstrasser, R. M., Ultrafast vibrational spectroscopy of a degenerate mode of guanidinium chloride. *The Journal of Physical Chemistry. B* **2009,** *113* (46), 15382-15391.

182. Vorobyev, D. Y.; Kuo, C.-H.; Kuroda, D. G.; Scott, J. N.; Vanderkooi, J. M.; Hochstrasser, R. M., Water-induced relaxation of a degenerate vibration of guanidinium using 2D IR echo spectroscopy. *The Journal of Physical Chemistry. B* **2010,** *114* (8), 2944-2953.